DYNAMIC RESPONSE OF GFRP LAMINATES WITH EMBEDDED PZT PATCHES

By

Raja Yellamaraju

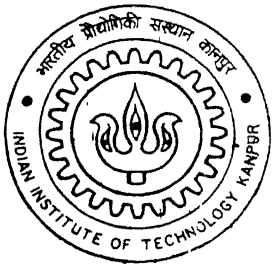

DEPARTMENT OF AEROSPACE ENGINEERING

Indian Institute of Technology Kanpur

FEBRUARY, 2002

DYNAMIC RESPONSE OF GFRP LAMINATES WITH EMBEDDED PZT PATCHES

A Thesis Submitted
In Partial Fulfillment of the Requirements
for the Degree of
Master of Technology

by

RAJA YELLAMARAJU

to the

DEPARTMENT OF AEROSPACE ENGINEERING
INDIAN INSTITUTE OF TECHNOLOGY KANPUR

FEBRUARY, 2002.

CERTIFICATE

It is certified that the work contained in the thesis entitled "***DYNAMIC RESPONSE OF GFRP LAMINATES WITH EMBEDDED PZT PATCHES***", by ***Raja Yellamaraju***, has been carried out under our supervision and that this work has not been submitted elsewhere for a degree.

Prof S.Kamle
Dept. of Aerospace Engineering
I.I.T Kanpur

Prof. N.G.R.Iyengar
Dept. of Aerospace Engineering
I.I.T. Kanpur

FEBRUARY, 2002

ACKNOWLEDGEMENT

I take this opportunity to express my immense gratitude and heartfelt thanks to Prof. Sudhir Kamle and Prof. N.G.R.Iyengar for their invaluable guidance, constant encouragement and advice at every stage of my thesis that made this work possible.

I am extremely indebted to Mr.B.Prasad and Mr Lavendra Singh of Aerostructure lab for assisting me in fabricating various set ups required for this work. I would like to thank Mr.B.K Jain of ACMS department, Mr.Diwakar of material testing lab and Mr.M.N Mungole of materials science lab for allowing me to use various facilities for successfully conducting the experiments.

My special regards to S.K.Muneshwar who helped me in experimental set up, Shanmukhi Gupta and to all my friends, who have made my stay at IIT Kanpur enjoyable.

Last, but not the least, I must express my deepest sense of gratitude to my grandpa,parents,mentors(Mr M.S Raju and Mr Y.M.Raju) for their constant support and encouragement.

Raju YRN.

Abstract

A smart laminated composite structure incorporates distributed actuators and sensors that are either surface bonded or embedded or both with the host structure and also includes onboard control and instrumentation.This work presents preparation of composite laminate from plain weave GFRP prepregs. The composite laminate was characterised by performing various tests to determine the four independent elastic constants.The smart glass/epoxy test specimen was manufactured with embedded PZT crystals. The test specimen was clamped on the fixture at one edge. The beam is connected to a magnetic shaker through a connecting rod at its other edge. The beam was subjected to a concentrated time varying(sinusoidal) load at its tip. The excitations of the beam were sensed by the embedded crystals. Accelerometer used as a sensor measures the response of the beam. The output of the crystals was amplified by using a charge amplifier and measured with the help of FFT Analyser. It was found that the response of the sensors were close to the theoretical estimates. Theoretical analysis was done by MSC Patran fem package.

Contents

List of Figures

List of Tables

Chapter 1

INTRODUCTION

1.1 GENERAL

The word composite means, "consisting of two or more distinct phases". Thus materials having two or more distinct constituents having distinct interface separating them are called composite materials. Composites can achieve certain physical properties not realizable by the constituent materials individually. These materials offer high specific strength and stiffness. Oriented fibrous composites also offer controlled anisotropy. The manufacture of composites requires comparatively low labor and generates less wastage in addition to the ease of processing of complicated structural forms. Composite structures are destined to many future applications, especially in Aerospace and transport industry due to their properties such as good fatigue and corrosion resistance, low heat conductivity, good electrical insulation properties, cost effectiveness, etc. In the recent past, extensive research on the manufacture, characterization, fatigue and fracture of these materials have increased the confidence in the use of these materials and thus composites have replaced conventional materials in many applications.

With progress in engineering design, increasing use is being made of lightweight high-strength materials. This is true irrespective of the field of their application whether it be buildings, bridges, Aerospace structures or mechanical structures. Spectacular progress has been witnessed in re-

cent years in a variety of scientific and engineering disciplines. In particular, metallic and composite materials and structural technology, computer aided structural design and analysis, microelectronics, microprocessors, sensors, signal processing, etc have seen rapid advancement. The synergistic interaction of these fields has lead to the birth of the new trans disciplinary field of Smart/Intelligent Structures Technology. Some have viewed these developments as the "dawn of a new materials and structures age!". 'Smart', 'Intelligent' and 'Adaptive' have all been used to describe and classify structures which contain their own sensors, actuators and control capabilities. The "smartness" or "intelligence" can be defined at three levels, each of them defining a field of research, technology development and potential applications:

- A material or a structure is said to be "sensitive" when it includes sensors providing information concerning the material itself or its environment. For instance the control of large and complex technological structures is a topic of rapidly growing interest.

- A material will be "adaptable" if integrated actuators (or "active" materials) can modify its characteristics. Such a material or structure will be adaptable only by the way of an externally determined action.

- The combination of these two above mentioned properties results in an "adaptive" or "really smart" material which collects data related to the changes in its environment or in its own evolution or damage. It processes these collected data, and reacts through its 'actuators' action.

1.2 Sensors and Actuators

Many types of sensors and actuators are being considered for introduction in smart systems. Typical sensors being used are of strain gauges, accelerometers, fiber optic sensors, piezoelectric films and piezoceramics. Sensors convert mechanical quantity (such as strain or displacement) into electric field.

Key factors for sensors are their sensitivity to strain or displacement , bandwidth and size. Other factors are temperature sensitivity, linearity, hysteresis, electromagnetic compatibility, embeddability and associated electronics.

Typical actuators are of piezoceramics, magnetostrictives, electrostrictives and shape memory alloys. Piezoelectrics and electrostrictives are available as ceramics, where as magnetostrictors and shape memory alloys are available as metal alloys. Most important performance parameters of actuators include maximum stroke or strain, maximum block force, stiffness and bandwidth. All these actuators directly convert actuating (electric/thermal) signals into actuation strain/displacement.

There has been some significant work investigating shape control and damage control of structures but not nearly to the extent of active and passive vibration control. Passive techniques utilize prior adjustment of the three design parameters - mass, stiffness and damping - to give a structure good dynamic response to an outside disturbance. These methods include tuning masses to place natural frequencies away from driving frequencies, vibration absorbers which create anti-resonance, and additional damping. Active control techniques allow for a much larger range of operating conditions Present active control schemes require the use of applied external forces or motion at discrete locations to oppose the vibration and effectively dissipate the energy in the structure. A structure with the ability to change its stiffness or damping in a controlled manner would offer an alternative to discrete external actuators. Smart structure applications are wide ranging from active shape control, vibration and noise control, improved damping, improved aeroelastic stability, to change of stress distribution. Many types of actuators and sensors are being considered, such as fiber optics, electro-rheological fluids, piezoelectric materials, shape memory alloys, electrostrictive materials, magnetostrictive materials, etc. These materials can be embedded in composite laminates and can be used as integral sensors or actuators.

1.3 Smart materials

The design of smart structure is significantly dependent on the appropriate selection of smart materials. The available smart materials can be classified into five major groups based on the characteristic working principles[1-3]. They are piezoelectric, magnetostrictive, shape memory, electro-rheological and magneto-rheological materials. Piezoelectric materials develop charge if deformed by the mechanical stress and by a converse effect, it deforms due to the application of electric field. A similar direct and converse relationship between mechanical and magnetic field exists for magnetostrictive material. Shape memory alloys have special features of memorizing a shape stretching, bending or twisting as a function of temperature and recovering that shape at different temperatures. They deform due to a phase change from martensite to austenite state. The phase transition is dependent on both stress and temperature such that by changing any one of them, volume change can be initiated. Electro-rheological fluids are a class of specially formulated colloidal suspensions, which undergo a change in the resistance to flow due to an electric field. Magneto-rheological fluids can be very effectively used for vibration suppression by building actuators out of this material.

The current generation of smart structures featuring piezoelectric materials is generally synthesized with polymeric fibrous composite laminates which readily accommodate embedded piezoelectric actuators and sensors. Any external force, applied on the beam will set vibrations and cause deformations in the beam. These deformations will cause stresses and strains in the beam. If the beam is embedded with smart crystals, these vibrations can be dampened quickly and deformations and resulting effects can be controlled to greater extent.

Among the various materials, the piezoelectric materials have proved to be the best for sensors and actuators in smart structures. Piezoelectrics undergo surface elongation when an electric field is applied across them and produce voltage when surface strain is applied and thus can be used both as actuators and sensors. Various commonly used actuation materials are the piezoelectric materials - Lead Zirconate Titanate (PZT), and Polyvinyli-

denefluoride (PVDF); ceramic electrostrictive material - Lead Magnesium Niobate (PMN); Terfenol, a rare earth magnetic like material and Nitinol (nickel titanium alloy) available in the form of wires or sheets. These substances have the ability to change the shape, natural frequency, damping and other mechanical characteristics of intelligent materials in response to a change in environment. When integrated into a structure either through embedding or surface bonding , they apply localized strains through which the deformation of the structural elements could be controlled. Due to their small size, a large number of piezoelectric actuator elements could be used without greatly increasing the mass of the structure.

LITERATURE REVIEW

The problem of exerting control on large or precision flexible structure has, in recent years, been the center of attraction of an exhaustive research effort through out the Aerospace engineering community [4]. Many presently planned and future missions such as structural health monitoring, vibration control, airfoil shape control, noise control, control surface actuation, smart radar, etc. need for pointing accuracy for better performance execution. World wide, many researchers have paid their attention towards the development of intelligent structures and have shown encouraging results in this field. The smart structure can help to reduce amplitude of vibration, bring down the overall mass, reduce drag on the wing and noise inside a fuselage, to name a few. They can be used on all Aerospace vehicles [5].

A detailed literature survey of the issues related to properties of PZT ceramics and their use as actuators for vibration control is not attempted in this chapter because of the extensive activity in this field. However, typical references are mentioned which provide some measure of background for the various issues of concern.

The actuators in a smart structure provide the mechanism for the structure to adapt to its surrounding by suppressing vibrations or changing the structure's shape. This requires an actuation authority over a broad bandwidth spectrum and over a wide range of displacement amplitudes (from tenths of micrometers to milli/centi meters).

Hagood et al [6] have shown that piezoelectric crystals can readily be embedded in composite structures without much affecting the global stiffness of the substructure and increasing the mass of the total system, to maximize the energy dissipation in the structure and exhibiting control on the vibrations. Another feature of their work is the development of suitable technique of embedding piezoelectric crystals in a composite laminate. They have shown that piezoelectrics are uniquely suited as elements of highly distributed sensors and actuators in smart structures.

Crawley and Luis [7] have investigated the use of piezoelectric actuators to excite steady-sate resonant vibrations in simple structural members such

as catilevered beams. The response of the specimens were found in good agreement with those predicted by the analytical models.

The feasibility of adopting piezoelectric films to detect damages in composites has been discussed by Shen et al [8]. In order to study the possibility of detecting and monitoring damage in composite laminates through piezoelectric film sensors, three different laminates in the presence of various damage were investigated and influence of damage on damage monitoring sensors was specifically analyzed.

Zhou et al [9] have presented a dynamic analytical approach for the design and integration of active piezoceramic (PZT) patch elements locally coupled with host structures. Several critical design issues have been addressed like determination of the actuator dynamic outputs, the prediction of energy conversion efficiency, the estimation of system power requirement and the limitation of induced alternate peak stress. Both the mechanical stress behaviour and the thermal stress characteristics of the PZT patch elements were investigated. The attention in parametric design was directed to the thickness and location of the elements.

Batra et al [10] have shown the determination of the optimum location of a given rectangular piezoelectric actuator that will require the minimum voltage to annul the deflection of a simply supported rectangular elastic plate vibrating near one of its fundamental frequencies.

Lee [11] presented theory of laminated piezoelectric plates for the design of distributed sensors/actuators. In his theory, the piezoelectric phenomenon to effect distributed control and sensing of bending, torsion, shearing, shrinking and stretching of a flexible plate has been developed. The theory is capable of modeling the electromechanical (actuating) and mechanoelectrical (sensing) behaviour of a laminate.

Padma Akella et al [12] studied the modeling and control issues related to smart structures bonded with piezoelectric sensors and actuators. They applied Hamilton's principle to obtain a linearized equation of motion. The natural modes are then found by solving an eigenvalue problem. Herman Shen [13] developed a one - dimensional theory for modeling the analysis of beams containing piezoelectric sensors and actuators. The equations of

motion and associated boundary conditions are derived for the vibrations of piezoelectrically sensored/actuated beams.

Chandrashekhara and Agarwal [14] presented a finite element formulation for modeling the behaviour of laminated composites with integrated piezoelectric sensors and actuators. This model is valid for both continuous and segmented piezoelectric elements that can be either surface bonded or embedded in the laminated plate. The formulation is based on the first order shear deformation theory, which is applicable for both thin and moderately thick plates. Liu et al [15] presented a finite element formulation to model the dynamic as well as static response of laminated composite plates containing integrated piezoelectric sensors and actuators subjected to both mechanical and electrical loadings.

Present Work

Investigations on dynamics of smart structures have been drawing attention of many researchers worldwide. Smart materials, may be defined as materials that posses the adaptive capabilities to external stimuli such as load or environment with inherent intelligence. The intelligence of the material could perhaps be programmed by material composition, processing, defect and microstructure or conditioning to adapt in a controlled manner to various levels of stimulus. Piezoelectric ceramic materials are typically employed as sensors and actuators. The objective of the current work are to perform various tests on the composite laminate to get the four independent constants and to study the vibration response of composite beam embedded with PZT crystals.

The various tests employed for characterising the laminate are described in Chapter 2. Formulation for free vibration response of the plate is given in Chapter 3. Theoretical analysis of beam vibration response is described in Chapter 4. Chapter 5 deals with the results, discussions, conclusions and suggestions for future work.

Chapter 2

PREPARATION OF LAMINATE

2.1 Basic Raw Materials:

The basic raw materials for the preparation of the laminate are the reinforcing material (glass woven fabric) and the matrix material (epoxy mixture).

2.1.1 Glass woven fabric

Woven fabrics are one of the most widely used reinforcing materials. Fabrics typically offer flexibility in fabrication techniques, but at a higher cost. Woven reinforcing fabrics are made by interlacing individual filaments, ends (untwisted fiber bundles), yarns (twisted fiber bundles), and rovings. Fabric composites have mechanical properties similar to those of laminates made from orthogonal unidirectional layers. Fabrics can be woven into many different types of weave patterns, widths and thicknesses. A variety of weave patterns can be used to interlace the warp and weft (filling) yarns to form a stable fabric. The major fabric styles are plain weaves, twills, satins and woven rovings. The plain weave, which interfaces one warp yarn over and under the weft (or filling) yarn, demonstrates the greatest degree of stability with respect to yarn slippage and fabric distortion (stability). Yarn count and content, however, also contribute to fabric stability. In the present work, plain weave fabric is used as the reinforcing material.

2.1.2 Epoxy Resin System

One of the most versatile properties of epoxy resins is their ability to transform readily from liquid state to tough, hard thermo-set solids. This hardening is accomplished by the addition of a chemically active reagent known as curing agent or hardener (sometimes requires heat and pressure). Accelerometers are sometimes added in catalytic amount to reduce the cure time. The specific resin-curing system will, to a very considerable extent, determine the ultimate properties of the laminate.

2.2 Composite Laminate for Dynamic Test

2.2.1 Specimen Preparation

Woven glass fiber cloth was used for making specimens for Dynamic and Tensile tests. The cloth was cut slightly larger than the required dimension into 19 layers. These are weighed to calculate the amount of epoxy required. 10% extra amount of the epoxy was added to make up the loss during lay up. Hand lay up technique was used to prepare the specimen. After lay up, the specimen was covered on top with a mylar sheet and a flat glass plate is placed on it. Weights were put on the glass surface and the extra matrix applied during the lay up was removed. Care should be taken while placing the weights, so that no slippage occurs between the layers. It was cured at room temperature for about 24 hours. The specimen was removed after curing and was cured in the oven at 100-120^o C for 2 to 3 hours. Final shape of the specimen was obtained by discarding the ends of the cured specimens. The size of the test specimen was 260 mm by 80 mm by 3.40 mm.

2.2.2 Embedding PZT Crystals into the Test Specimen

To accommodate the PZT disc's in the laminate, fibers from that particular location should be removed. The size of the crystal was 10 mm by 10 mm by 0.25 mm. Lead wire of diameter 0.2 mm was soldered on both faces of the crystal. The holes are made 1 mm greater than the size of the PZT crystals.

Two crystals are used and each is placed at equi-distance from the mid layer of the laminate at a distance of one - fourth the length from one edge and at the centre of plate width. The specimen with the embedded crystals is shown in the Fig.2.1.

2.3 Characterization Of Composite Laminate

2.3.1 Tensile Test

Tensile modulus of the composite laminate was first determined by the tensile test, performed on the specimens prepared as per the ASTM D3039-76 [16] standard specifications. The properties deduced from the tension tests on composite materials are effective (average) properties. The test method (ASTM D3039-76) applies to unidirectional laminates but can also be performed on multi-directional laminates, woven fabrics, or discontinuous fiber composites.

Specimen Preparation

The most commonly used specimen geometries are the dog-bone specimen and flat specimen with end tabs. In the present work, flat specimens are used. The standard specimen used for the determination of the Young's Modulus in the longitudinal direction of the composite laminate is shown in figure. Five specimens of same dimensions are used for the test.

Woven glass cloth was cut into number of pieces required for the given thickness. The cloth was cut into the rectangular pieces of the size 230 mm by 150 mm. 18 plies were used to achieve the required thickness. Resin is heated to 70 - 80 °C and cooled to room temperature. Once it is cooled, 9 - 10 parts by weight of the hardener is mixed thoroughly until even distribution was achieved. Once it is mixed, the prepared mixture is used without delay since the pot life of the mixture is about 0.5 - 1 hour. The Resin - Hardener ratio is given in Table 2.1

Two flat glass plates of size 500 mm by 500 mm by 5 mm are used for laying the specimen. One plate is placed on a smooth surface with a mylar

sheet of same area on it. Hand lay up technique is used for the specimen preparation. The epoxy mixture is applied on each layer of the lamina with a brush and stacked evenly. Once all the plies are stacked, one more mylar sheet is placed on it. The other glass is placed on the top this mylar sheet. Weights are placed on the top surface of the glass for pressure. Extra resin applied during lamination could be drained out when pressure is applied over the laminate. Curing was carried out at room temperature for about 24 hours and then semi-cured laminate was transferred to the oven, where it was held at 100 - 110 °C for about 1 - 2 hours. Finally, the end parts are discarded and the five specimens of required size are cut from the laminate. The tensile test specimen is shown in Fig.2.2.

Points to be cared during specimen preparations are:

1. All the surfaces must be flat, any irregularity should be avoided.
2. Resin, if needed, should be heated to 70 - 80 °C to avoid moisture trapping before mixing with hardener.
3. PVA solution must be applied over the surfaces of every part.
4. Pressure should be applied uniformly on the laminate to reduce the non-uniformity in thickness.
5. Specimen must be symmetric with respect to centre line.

Testing Procedure

The tensile test of all the five specimens was carried out on a MTS - 810 machine. The tests were done in the load control mode. The specimen was clamped between the hydraulic grips and aligned correctly. Load was applied at the rate of 0.4 ton/min. An extensometer (MTS 632 - 25C - 20) was used to measure the strain.

A typical load vs strain curve for the specimen is shown in Fig.2.3. The data obtained from the test was analysed to estimate the strength and elastic modulus of the laminate.

2.3.2 Burn out test

Burn out test was carried out to calculate the exact fiber fraction in the laminate and finding out the various properties of the laminate by applying the rule of mixtures. The significance of this method [17] is it can be used to obtain the ignition loss of a cured reinforced resin sample. If only glass fabric is used as the reinforcement of an organic resin that is completely decomposed to volatile materials under the conditions of this test and the small amount of volatiles (water, residue solvent) that may be present is ignored, the ignition loss can be considered to be the resin content of the samples. This method does not provide a measure for resin content of the samples containing reinforce materials that lose weight under the conditions of the test or containing resin that does not decompose to volatiles materials released by ignition.

Apparatus

Crucible ceramic crucibles were used. Electric furnace, variac controlled electric furnace capable of maintaining 1350 °C was used for this test.

Test Specimen

For the sake of homogeneity, samples were cut from the specimens that had been used for mechanical properties determination. The fractured areas were removed and three specimens of the sizes given in Table 2.2 were prepared.

Thickness of all the specimens was 3.10 mm.

Procedure

The crucibles were heated to 500 to 600° C for 15 minutes or more, cooled to room temperature in a desiccator and weighed to the nearest 0.1 mg. The composite specimens were also weighed to the nearest 0.1 mg. Then they were placed in the respective crucibles. Weight of all the crucibles, the specimens and the weight of the crucible with specimen before and after test are summarized in the Table 2.3

Crucibles and the contents were placed in the furnace and the temperature was raised up to 600° C. they were held at this temperature for 6 hours, the time until all carbonaceous material has disappeared. They were then cooled to room temperature in the desiccator and weighed to the nearest 0.1 mg. Since weight of the fiber and matrix and density of both the fiber and matrix are known, one can easily calculate the volume fraction of fiber. The volume fraction of the fiber was found to be 0.46 on average. The difference in fiber fraction of the various samples was within 0.8%. The density of the laminate was 1 643 gm/cm3.

2.3.3 Inplane Shear Test

Test Method

Inplane shear properties of a composite can be determined by conducting a tension test on a $[\pm 45^o]_s$ glass/epoxy fabric laminate The test results are interpreted by carrying out stress analysis of the laminate. For an applied stress σ_x, we have,

$$\tau_{LT} = \frac{\sigma_x}{2}$$

and

$$\sigma_x = \frac{F}{(b \times d)}$$

The inplane shear strength is, therefore,

$$\tau_{LT} = \frac{F}{2 \times (b \times d)}$$

where F is the failure load in Kilo Newton (KN), b and d are the cross-sectional dimensions of the specimen in mm

The lamina strains are related to the laminate strains as follows:

$$\gamma_{LT} = \left(\epsilon_x^o - \epsilon_y^o\right)$$

The inplane shear modulus is, therefore,

$$G_{LT} = \frac{\tau_{LT}}{\gamma_{LT}}$$

$$= \frac{F}{2 \times (b \times d) \times \left(\epsilon_x^o - \epsilon_y^o\right)}$$

The Mohr circle for stresses and strains are shown in Fig.2.4 and Fig.2.5 respectively.

Specimen dimensions

The geometry of the $[\pm 45^o]_{4s}$ tensile off-axis is shown in Fig.2.6. Two specimens were used for testing. The size of the specimens were $(190 \times 25 \times 2.65) mm$. The end tabs were of aluminium. The size of end tabs were $(40 \times 25 \times 2)\, mm$.

Test Procedure

For characterizing the material, tension tests were performed. The test was carried out on Table Top Tensile Testing Machine (Hounsfield Test Machine - W series: Maximum load - 20 KN) . The specimen is first aligned in the grips and tightened in place. The specimen was then loaded at a constant rate of 1.5 mm/min. The applied load was measured from the display menu on the machine. In order to determine the specimen strains, strain gauges were mounted on the specimen and monitored during the test. Strain gauges with resistance of 120 $\pm 0.2\ \Omega$ were used. Two gauges were applied to each specimen in the longitudinal and transverse to the loading direction. The gauges were located close to the geometric centre of the specimen. The gauge reading was measured with the help of a multi channel strain indicator. A stress-strain diagram is drawn from the test data and shown in Fig.2.7. From the data, the value of inplane shear modulus was calculated.

Table 2.1: RESIN HARDNER RATIO

	Parts by weight
Araldite CY 230	100
Hardner HY 951	9 - 10

Table 2.2: BURN OUT TEST SPECIMENS SIZE

S.No	Size of the Specimen (mm x mm)
1	2.00 x 2.15
2	2.05 x 2.15
3	2.00 x 2.20

Table 2.3: WEIGHT OF THE SPECIMEN BEFORE AND AFTER BURN OUT TEST

S.No	Specimens wt. (gm)	Crucibles wt. (gm)	Crucibles wt. with specimen (gm) (before test)	Crucibles wt. with specimen (gm) (after test)
1	2.1459	45.9964	48.1423	47.2033
2	2.2437	37.3942	39.6379	38.6390
3	2.2885	41.8910	44.1795	43.1620

2.3.4 Determination of Poisson's Ratio

The size of the specimen used was 160 mm by 25 mm by 3.10 mm. Strain gauges were applied in longitudinal and transverse direction at equi-distant from centre of the specimen. The specimen is aligned in place between the grips of the machine. The strain gauge readings were recorded by a multi-channel strain indicator. Poisson ratio was calculated by dividing lateral strain by longitudinal strain.

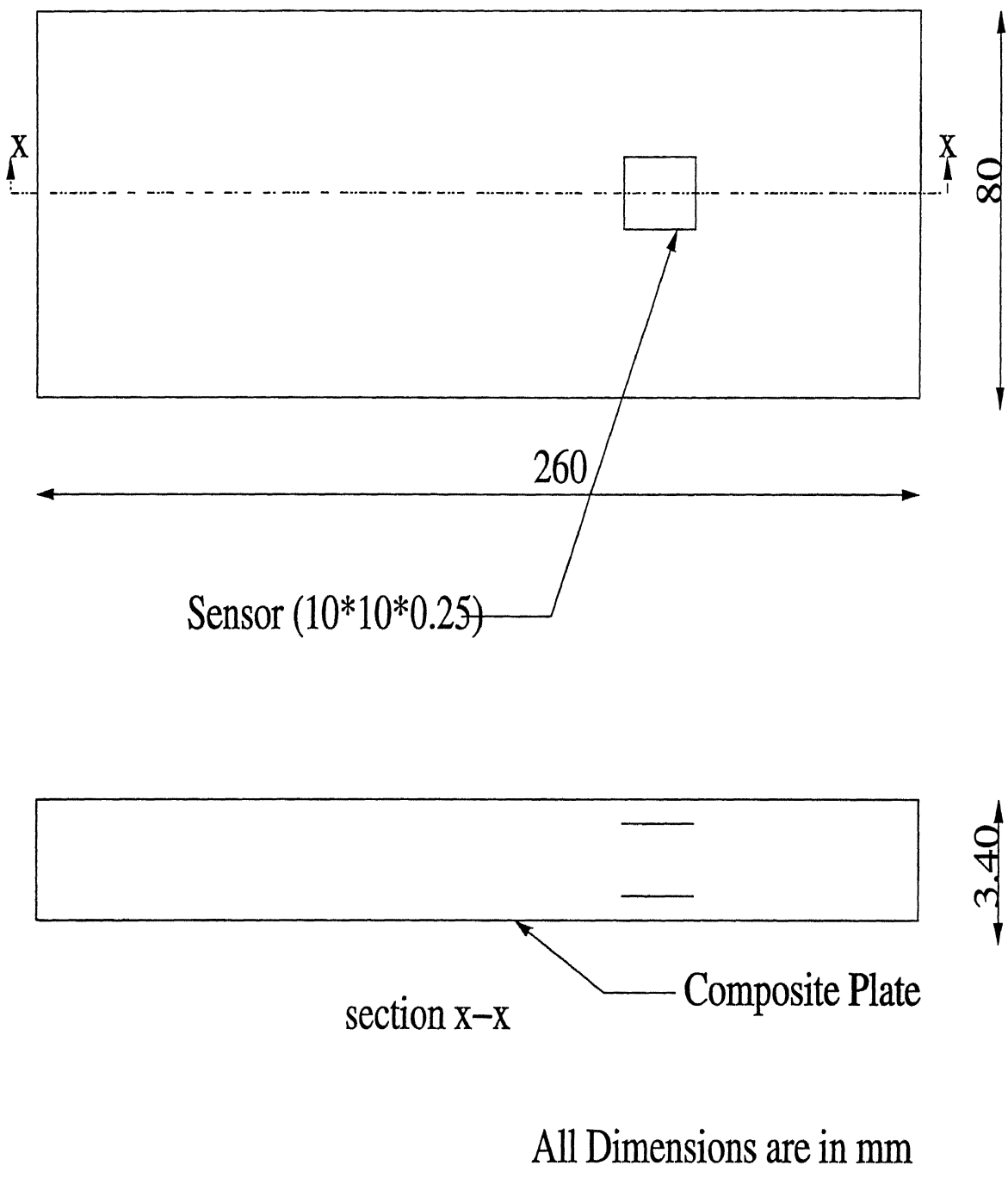

Figure 2.1: DYNAMIC TEST SPECIMEN

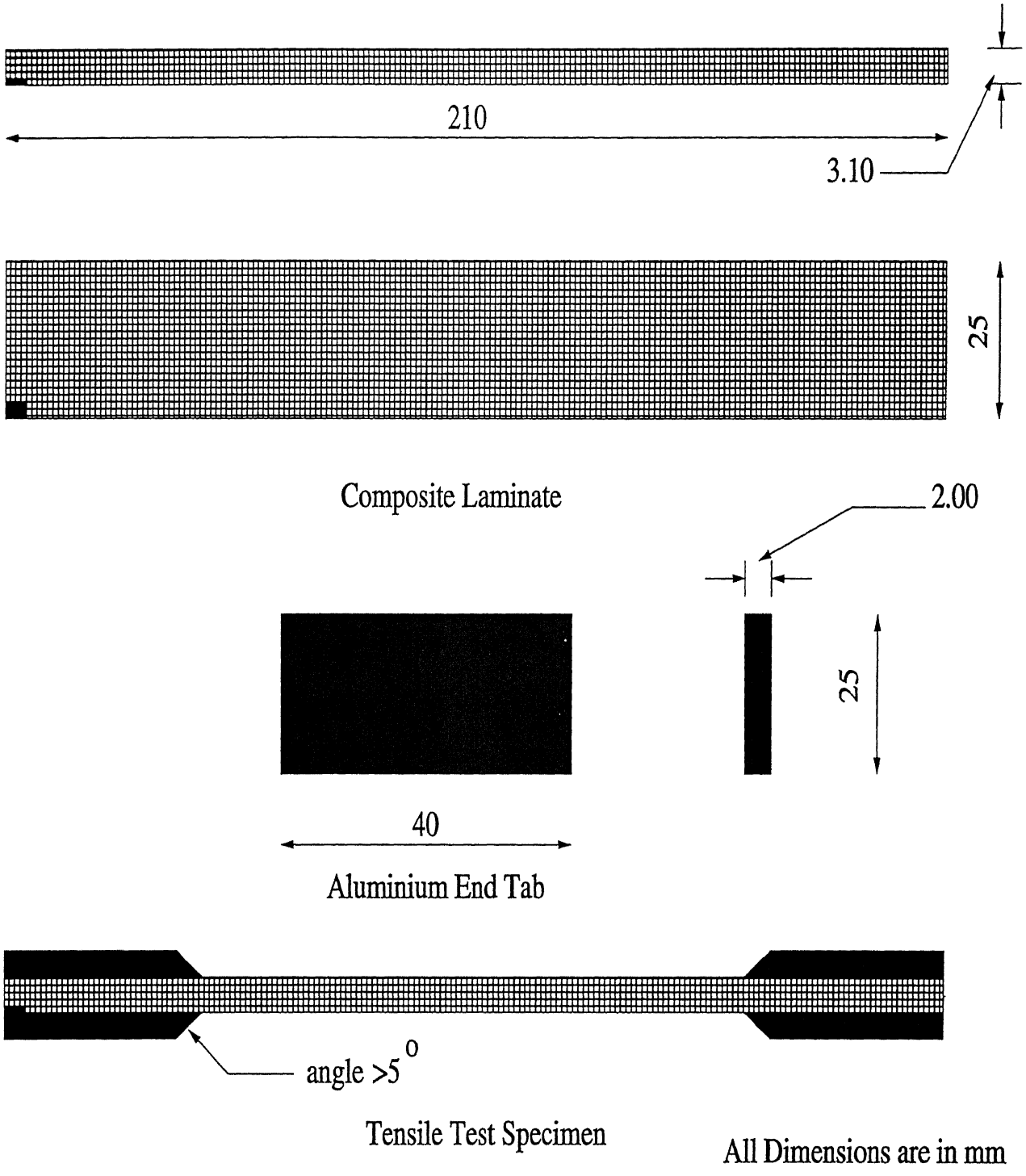

Figure 2.2: TENSILE TEST SPECIMEN

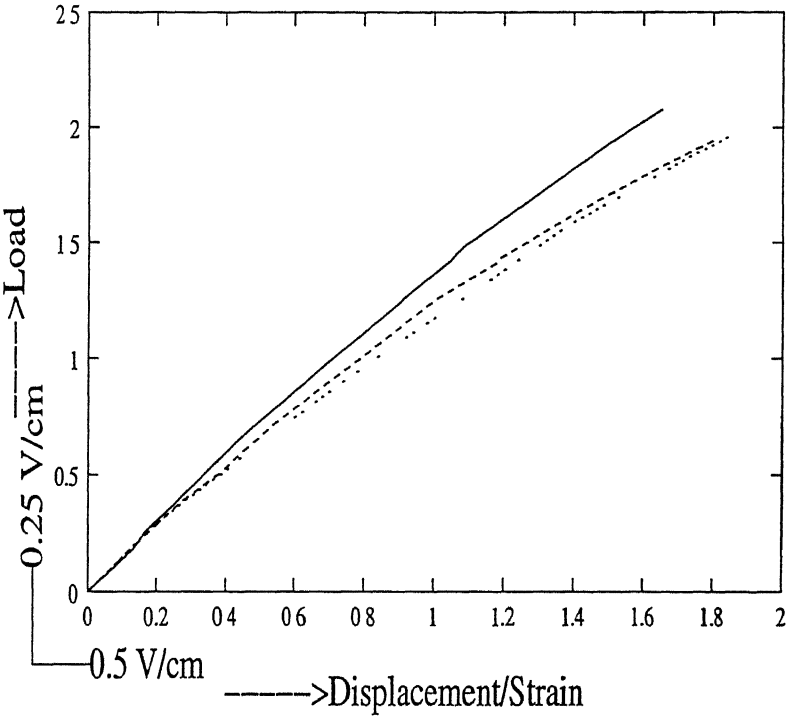

Gauge Length = 50 mm

Load 100% (10 V = 10,000 kg)

Strain 50% (10 V = 12.5 mm displacement or 0.250 strain)

Stroke 10% (10 V = 10 mm)

Figure 2.3: A TYPICAL LOAD VS STRAIN CURVE FOR TENSILE TEST

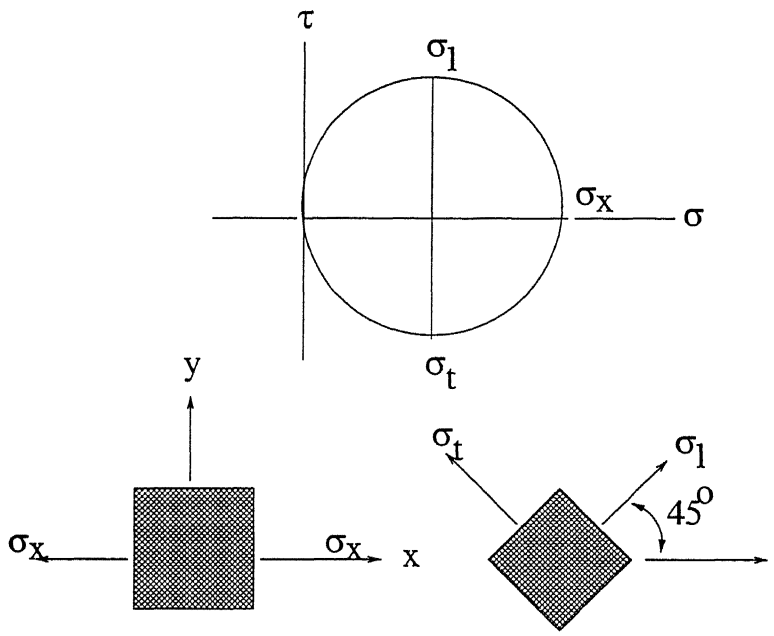

Figure 2.4: MOHR CIRCLE DIAGRAM FOR STRESSES IN INPLANE SHEAR TEST

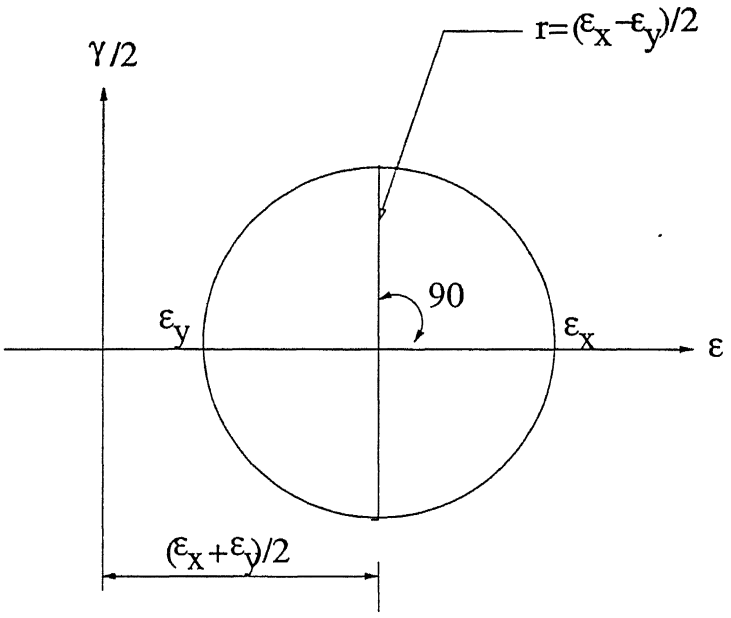

Figure 2.5: MOHR CIRCLE DIAGRAM FOR STRAINS IN INPLANE SHEAR TEST

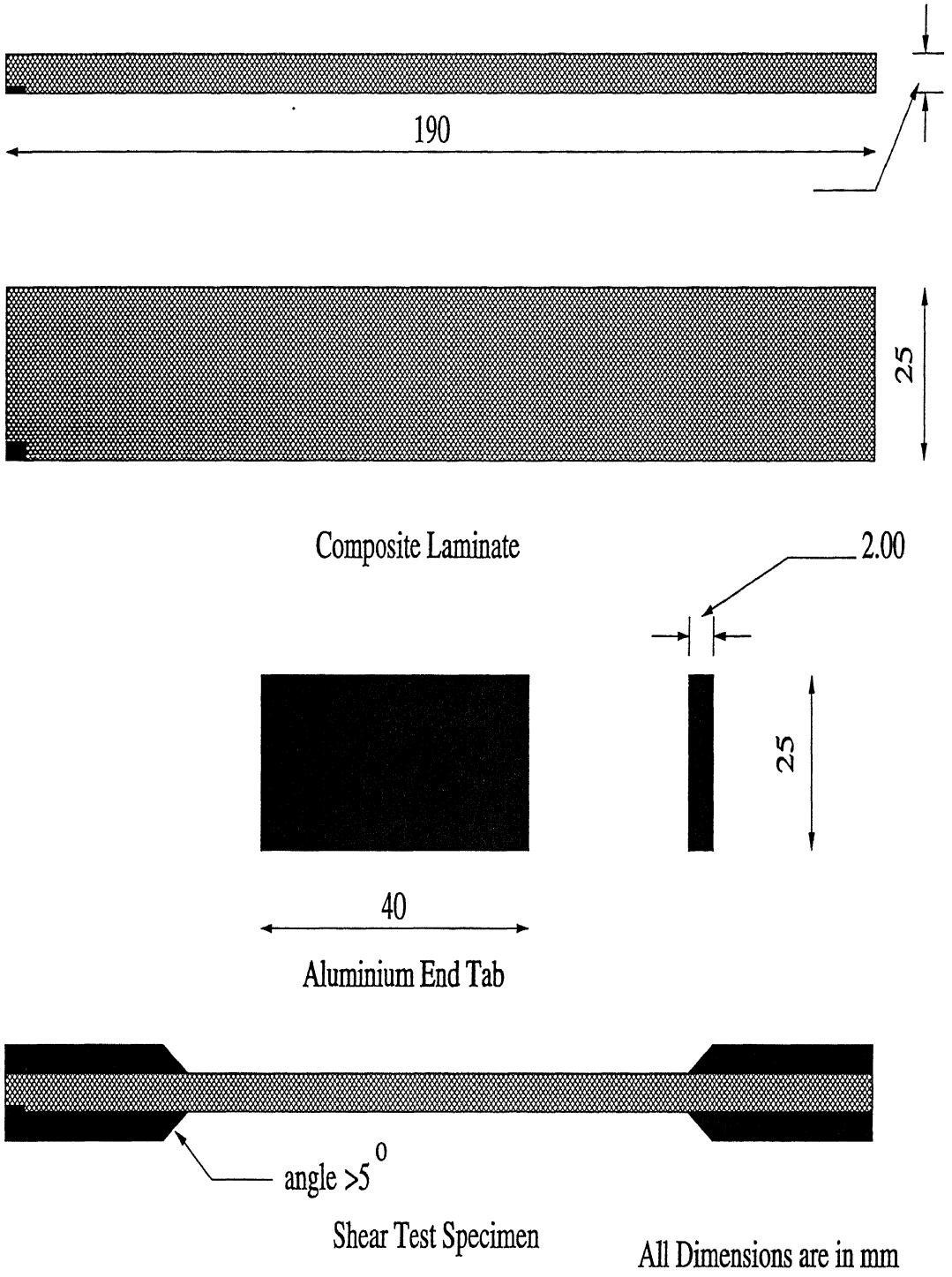

Figure 2.6: [$\pm 45^o$] TEST SPECIMEN FOR INPLANE SHEAR TEST

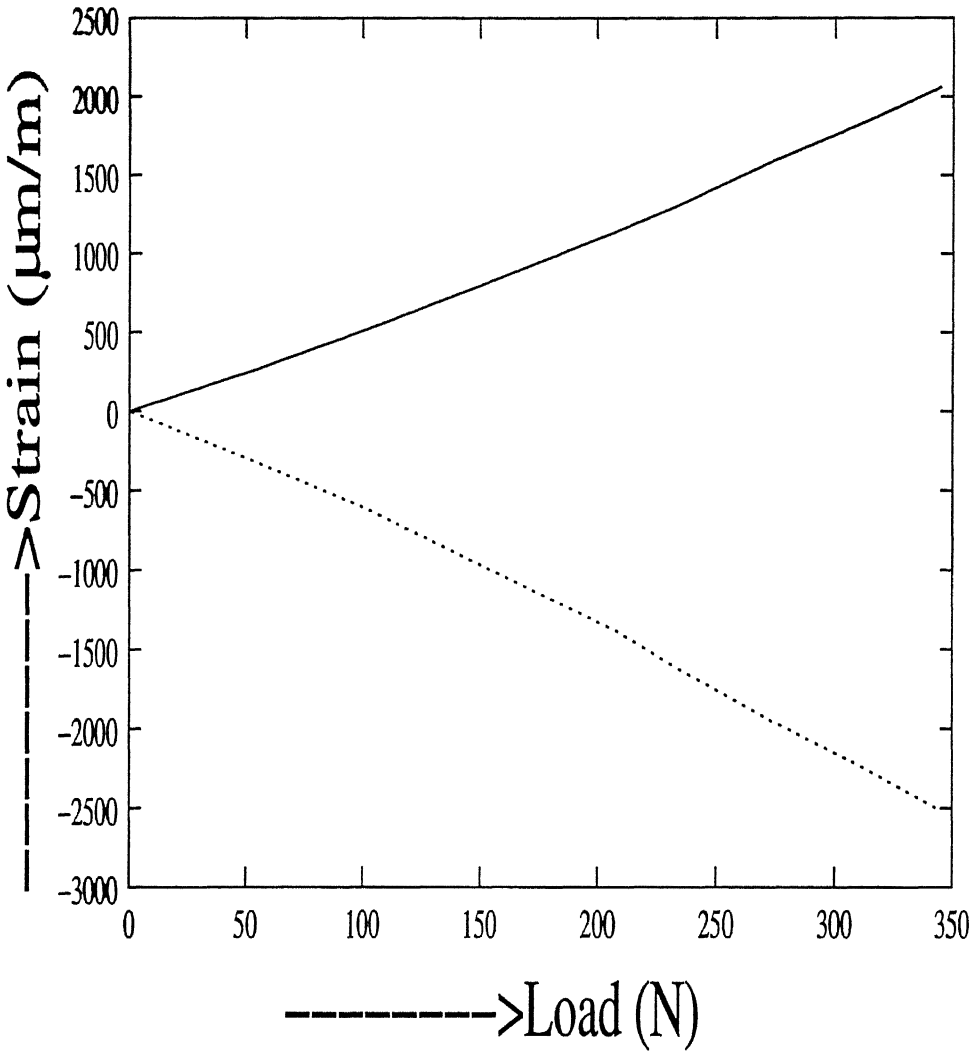

Figure 2.7: A TYPICAL LOAD VS STRAIN CURVE FOR INPLANE SHEAR TEST

Chapter 3

FORMULATION FOR FREE VIBRATION

The problem is formulated for a fiber - reinforced laminated composite rectangular plate of length a, width b, and thickness h composed of orthotropic layers of thickness h_z with fibers oriented at angles θ and -θ as shown in figure 3.1.

Certain assumptions made for the finite element formulation were:

1. The area and mass of the actuator embedded in the plate is negligible compared to that of the plate.

2. Equations for actuator and sensor were not considered.

3.1 Strain-Displacement Relations

The displacement field based on a first - order shear deformation theory is given by (Yang et al. [18])

$$u(x,y,z,t) = u^o(x,y,t) + z\psi_x(x,y,t)$$

$$v(x,y,z,t) = v^o(x,y,t) + z\psi_y(x,y,t) \tag{3.1}$$

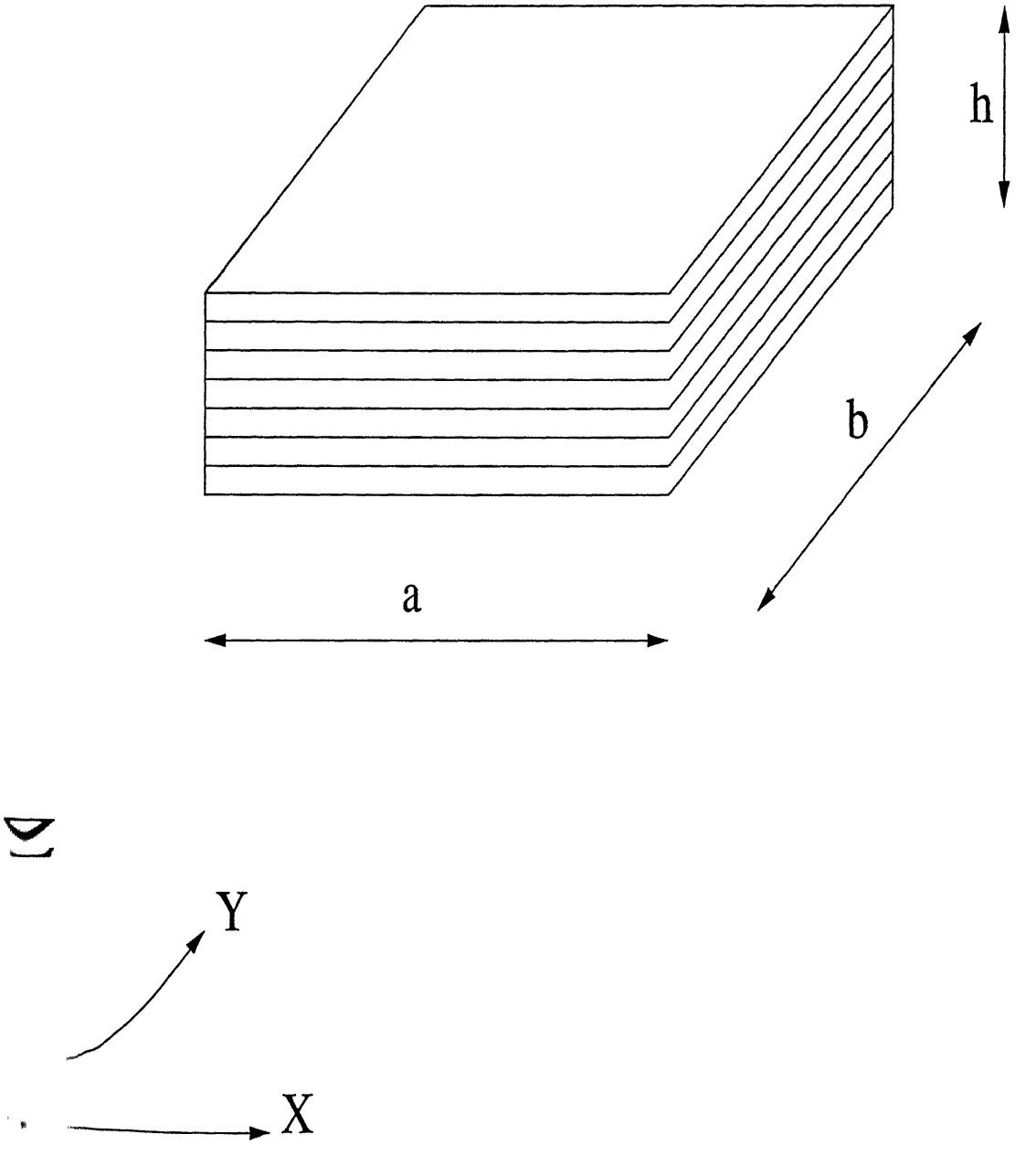

Figure 3.1: PLATE REPRESENTATION

$$w(x, y, z, t) = w^o(x, y, t)$$

where u, v, and w are the displacement components in the x, y, and z directions, respectively, t is the time, u^o, v^o, and w^o are the in - plane and transverse displacements of a point (x,y) on the mid-plane, respectively, ψ_x and ψ_y are the rotations of the normal to the mid-plane about the y and x axes, respectively.

Equation 3.1 can be expressed in matrix notation as

$$\{u\} = [G]\{\overline{u}\} \tag{3.2}$$

where

$$\{u\} = (u, v, w)^T \tag{3.3}$$

$$\{\overline{u}\} = (u^o, v^o, w^o, \psi_x, \psi_y)^T \tag{3.4}$$

$$[G] = \begin{bmatrix} 1 & 0 & 0 & z & 0 \\ 0 & 1 & 0 & 0 & z \\ 0 & 0 & 1 & 0 & 0 \end{bmatrix} \tag{3.5}$$

Substituting Equation 3.1 into infinitesimal strain relations, we can write

$$\{\epsilon\} = \{\epsilon^o\} + z\{\chi\} \tag{3.6}$$

where

$$\{\epsilon\} = (\epsilon_x, \epsilon_y, \epsilon_z, \gamma_{xy}, \gamma_{xz}, \gamma_{yz})^T \tag{3.7}$$

$$\{\epsilon^o\} = (\epsilon^o_x, \epsilon^o_y, 0, \gamma^o_{xy}, \gamma^o_{xz}, \gamma^o_{yz})^T$$

$$= \left(\frac{\partial u^o}{\partial x}, \frac{\partial v^o}{\partial y}, 0, \frac{\partial u^o}{\partial y} + \frac{\partial v^o}{\partial x}, \frac{\partial w^o}{\partial x} + \psi_x, \frac{\partial w^o}{\partial y} + \psi_y \right)^T \tag{3.8}$$

$$[\chi] = (\chi_x, \chi_y, 0, \chi_{xy}, 0, 0)^T$$

$$= \left(\frac{\partial \psi_x}{\partial x}, \frac{\partial \psi_y}{\partial y}, 0, \frac{\partial \psi_x}{\partial y} + \frac{\partial \psi_y}{\partial x}, 0, 0 \right)^T \tag{3.9}$$

The generalized strain vector $\{\overline{\epsilon}\}$ corresponding to the mid-plane can be defined as

$$\{\overline{\epsilon}\} = \left(\epsilon_x^o, \epsilon_y^o, \gamma_{xy}^o, \gamma_{xz}^o, \gamma_{yz}^o, \chi_x, \chi_y, \chi_{xy} \right)^T \tag{3.10}$$

which can be written as

$$\{\overline{\epsilon}\} = [L]\,\{\overline{u}\} \tag{3.11}$$

where $[L]$ is a derivative operator matrix defined by

$$[L] = \begin{bmatrix} d_x & 0 & 0 & 0 & 0 \\ 0 & d_y & 0 & 0 & 0 \\ d_y & d_x & 0 & 0 & 0 \\ 0 & 0 & d_x & 1 & 0 \\ 0 & 0 & d_y & 0 & 1 \\ 0 & 0 & 0 & d_x & 0 \\ 0 & 0 & 0 & 0 & d_y \\ 0 & 0 & 0 & d_y & d_x \end{bmatrix} \tag{3.12}$$

where

$$d_x = \frac{\partial}{\partial x} \qquad and \qquad d_y = \frac{\partial}{\partial y} \tag{3.13}$$

3.2 Stress strain relations for an orthotropic lamina

Stress strain relations for a lamina in the material coordinate axis, whose fibers are oriented at an angle α with reference to the $x - axis$ is given as [19-21]

$$\begin{Bmatrix} \sigma_1 \\ \sigma_2 \\ \tau_{12} \\ \tau_{13} \\ \tau_{23} \end{Bmatrix} = \begin{bmatrix} Q_{11} & Q_{12} & 0 & 0 & 0 \\ Q_{21} & Q_{22} & 0 & 0 & 0 \\ 0 & 0 & Q_{66} & 0 & 0 \\ 0 & 0 & 0 & Q_{44} & 0 \\ 0 & 0 & 0 & 0 & Q_{55} \end{bmatrix} \begin{Bmatrix} \epsilon_1 \\ \epsilon_2 \\ \gamma_{12} \\ \gamma_{13} \\ \gamma_{23} \end{Bmatrix} \tag{3.14}$$

where $\sigma_1, \sigma_2, \epsilon_1, and\, \epsilon_2$ are stresses and strains in the direction parallel and perpendicular to the fiber direction,$\tau_{12}, \tau_{13}, \tau_{23}, \gamma_{12}, \gamma_{13}, and\, \tau_{23}$ are shear stresses and shear strains in the respective directions.

The stiffness coefficients $Q_{11}, Q_{22}, ..., etc.$, are defined in terms of material properties as

$$Q_{11} = \frac{E_1}{(1 - \nu_{12}\nu_{21})},$$

$$Q_{12} = \frac{\nu_{21}E_1}{(1 - \nu_{12}\nu_{21})},$$

$$Q_{21} = Q_{12},$$

$$Q_{22} = \frac{E_2}{(1 - \nu_{12}\nu_{21})}, \tag{3.15}$$

$$Q_{66} = G_{12},$$

$$Q_{44} = G_{13},$$

$$Q_{55} = G_{23}.$$

3.3 Laminate Constitutive Relations

The stresses and strains in x, y and z directions are obtained by transforming the relation given in Equation 3.14. The transformed stress-strain relations for a k^{th} lamina are given as

$$\begin{Bmatrix} \sigma_x \\ \sigma_y \\ \tau_{xy} \\ \tau_{xz} \\ \tau_{yz} \end{Bmatrix}_k = \begin{bmatrix} \overline{Q}_{11} & \overline{Q}_{12} & \overline{Q}_{16} & 0 & 0 \\ \overline{Q}_{21} & \overline{Q}_{22} & \overline{Q}_{26} & 0 & 0 \\ \overline{Q}_{16} & \overline{Q}_{26} & \overline{Q}_{66} & 0 & 0 \\ 0 & 0 & 0 & \overline{Q}_{44} & \overline{Q}_{45} \\ 0 & 0 & 0 & \overline{Q}_{54} & \overline{Q}_{55} \end{bmatrix}_k \begin{Bmatrix} \epsilon_x \\ \epsilon_y \\ \gamma_{xy} \\ \gamma_{xz} \\ \gamma_{yz} \end{Bmatrix}_k \tag{3.16}$$

where

$$\overline{Q}_{11} = Q_{11}m^4 + 2(Q_{12} + 2Q_{66})m^2n^2 + Q_{22}n^4,$$

$$\overline{Q}_{12} = (Q_{11} + Q_{22} - 4Q_{66})m^2n^2 + Q_{12}(m^4 + n^4),$$

$$\overline{Q}_{22} = Q_{11}n^4 + 2(Q_{12} + 2Q_{66})m^2n^2 + Q_{22}m^4,$$

$$\overline{Q}_{16} = (Q_{11} - Q_{12} - 2Q_{66})m^3n + (Q_{12} - Q_{22} + 2Q_{66})mn^3,$$

$$\overline{Q}_{26} = (Q_{11} - Q_{12} - 2Q_{66})mn^3 + (Q_{12} - Q_{22} + 2Q_{66})m^3n,$$

$$\overline{Q}_{66} = (Q_{11} + Q_{22} - 2Q_{12} - 2Q_{66})m^2n^2 + Q_{66}(m^4 + n^4),$$

$$\overline{Q}_{44} = Q_{44}m^2 + Q_{55}n^2,$$

$$\overline{Q}_{45} = (Q_{44} - Q_{55})mn,$$

$$\overline{Q}_{55} = Q_{55}m^2 + Q_{44}n^2.$$

where

$$m = \cos\alpha \qquad and \qquad n = \sin\alpha$$

Using the above lamina constitutive equations, the laminate constitutive relations can be written as

$$\left\{\overline{N}\right\} = \left[\overline{D}\right]\{\overline{\epsilon}\} \tag{3.17}$$

where $\left\{\overline{N}\right\}$ is the stress and moment resultant vector corresponding to the mid-plane defined by

$$\left\{\overline{N}\right\} = (N_x, N_y, N_{xy}, M_x, M_y, M_{xy}, Q_x, Q_y)^T \tag{3.18}$$

$$(N_x, N_y, N_{xy}, Q_x, Q_y) = \int_{-h/2}^{h/2} (\sigma_x, \sigma_y, \tau_{xy}, \tau_{xz}, \tau_{yz})\, dz$$

$$(M_x, M_y, M_{xy}) = \int_{-h/2}^{h/2} (\sigma_x, \sigma_y, \tau_{xy})\, z dz$$

$$\left[\overline{D}\right] = \begin{bmatrix} A_{11} & A_{12} & A_{16} & B_{11} & B_{12} & B_{16} & 0 & 0 \\ A_{21} & A_{22} & A_{26} & B_{21} & B_{22} & B_{26} & 0 & 0 \\ A_{16} & A_{26} & A_{66} & B_{16} & B_{26} & B_{66} & 0 & 0 \\ B_{11} & B_{12} & B_{16} & D_{11} & D_{12} & D_{16} & 0 & 0 \\ B_{21} & B_{22} & B_{26} & D_{21} & D_{22} & D_{26} & 0 & 0 \\ B_{16} & B_{26} & B_{66} & D_{16} & D_{26} & D_{66} & 0 & 0 \\ 0 & 0 & 0 & 0 & 0 & 0 & A_{44} & A_{45} \\ 0 & 0 & 0 & 0 & 0 & 0 & A_{54} & A_{55} \end{bmatrix} \tag{3.19}$$

$$(A_{ij}, B_{ij}, D_{ij}) = \sum_{k=1}^{N} \int_{z_{k-1}}^{z_k} \overline{Q}_{ij}^{k}(1, z, z^2)dz \qquad (i, j = 1, 2, 6)$$

$$A_{ij} = \sum_{k=1}^{N} \int_{z_{k-1}}^{z_k} \overline{Q}_{ij}^{k} dz \qquad (i, j = 4, 5) \tag{3.20}$$

3.4 Energy equations

Hamilton's variational principle is used to derive the laminate equations of motion. The mathematical statement of Hamilton's principle in the absence of damping can be written as

$$\int_{t1}^{t2} (\delta K - \delta U + \delta W)\, dt = 0 \tag{3.21}$$

where K is the kinetic energy, U is the strain energy, and W is the potential energy of prescribed surface tractions.

The kinetic energy term is

$$\delta K = \int_V \rho \{\delta\, \dot{u}\}^T \{u\}\, dV \tag{3.22}$$

where

$\{\dot{u}\} = \partial \{u\} / \partial t$ is the velocity vector of any generic point (x, y, z) in space, ρ is the mass density of the material, and V is the volume of the plate.

Differentiating Equation 3.2 with respect to time, substituting into Equation 3.22, and carrying out the integration through the thickness of the laminate, we get

$$\delta K = \int_A \left\{\delta\, \dot{\bar{u}}\right\}^T \left[\overline{M}\right] \left\{\dot{\bar{u}}\right\} dA \tag{3.23}$$

where

$$\left[\overline{M}\right] = \int_{-h/2}^{h/2} \rho\, [G]^T [G]\, dz$$

$$= \begin{bmatrix} I_1 & 0 & 0 & I_2 & 0 \\ 0 & I_1 & 0 & 0 & I_2 \\ 0 & 0 & I_1 & 0 & 0 \\ I_2 & 0 & 0 & I_3 & 0 \\ 0 & I_2 & 0 & 0 & I_3 \end{bmatrix} \tag{3.24}$$

where I_1, I_2, and I_3 are the normal, coupled normal - rotary and rotary inertia coefficients defined by

$$(I_1, I_2, I_3) = \sum_{k=1}^{N} \int_{z_{k-1}}^{z_k} \rho_k \left(1, z, z^2\right) dz$$

The strain energy term is

$$\delta U = \int_V \{\delta\epsilon\}^T \{\sigma\}\, dV \tag{3.25}$$

Integrating above equation through the laminate thickness, gives

$$\delta U = \int_A \{\delta\bar{\epsilon}\}^T \left\{\overline{N}\right\} dA \tag{3.26}$$

Substituting Equation 3.17 into the above equation, gives

$$\delta U = \int_A \{\delta\bar{\epsilon}\}^T \left[\overline{D}\right] \{\bar{\epsilon}\}\, dA \tag{3.27}$$

For free vibration analysis, the potential energy

$$\delta W = 0 \tag{3.28}$$

Substituting Equations 3.23, 3.27, and 3.28 into Equation 3.21, we get

$$\int_{t1}^{t2} \int_A \left[\left\{ \delta \, \overline{u} \right\}^T \left[\overline{M} \right] \left\{ \overline{u} \right\} - \left\{ \delta \overline{\epsilon} \right\}^T \left[\overline{D} \right] \left\{ \overline{\epsilon} \right\} \right] dA dt = 0 \tag{3.29}$$

Integrating the first term by parts, the above equation can be written as

$$\int_{t1}^{t2} \int_A \left[\left\{ \delta \overline{u} \right\}^T \left[\overline{M} \right] \left\{ \ddot{\overline{u}} \right\} + \left\{ \delta \overline{\epsilon} \right\}^T \left[\overline{D} \right] \left\{ \overline{\epsilon} \right\} \right] dA dt = 0 \tag{3.30}$$

3.5 Finite Element Formulation

The finite element formulation is based on the first order shear deformation theory. The plate is divided into a number of isoparametric four-noded quadrilateral elements with five degrees of freedom(DOF) per node $(u^o, v^o, w^o, \psi_x, \psi_y)$. Linear interpolation functions for all variables over each element was taken. Accordingly, the displacement vector at any node within the element is expressed as

$$\left\{ \overline{u}^e(x, y, t) \right\} = \sum_{i=1}^{NN} \left[N_i^e(x, y) \right] \left\{ \overline{u}_i^e(t) \right\} \tag{3.31}$$

where NN is the number of nodes per element and

$$\left[N_i^e \right] = N_i^e \left[I \right]$$

$$\left\{ \overline{u}_i^e \right\} = \left(u_i^o, v_i^o, w_i^o, \psi_{xi}, \psi_{yi} \right)^T$$

Here, N_i^e are the element shape functions, $[I]$ is a 5×5 identity matrix, and $u_i^o, v_i^o, w_i^o, \psi_{xi}$ and ψ_{yi} are the nodal values of u^o, v^o, w^o, ψ_x and ψ_y, respectively . The superscript e denotes the parameter at element level.

Equation 3.31 can also be written as

$$\{\overline{u}^e\} = [N^e]\{a^e\} \tag{3.32}$$

where

$$[N^e] = [[N_1^e], [N_2^e], ..., [N_{NN}^e]]$$

$$\{a^e\} = \left(\{\overline{u}_1^e\}^T, \{\overline{u}_2^e\}^T, ..., \{\overline{u}_{NN}^e\}^T\right)^T$$

Substituting Equation 3.32 into Equation 3.11, we get

$$\{\overline{\epsilon}^e\} = [B^e]\{a^e\} \tag{3.33}$$

where

$$[B^e] = [L][N^e] \tag{3.34}$$

B^e is the strain displacement matrix in terms of shape functions and is given as

$$[B_i^e] = \begin{bmatrix} \frac{\partial N_i}{\partial x} & 0 & 0 & 0 & 0 \\ 0 & \frac{\partial N_i}{\partial y} & 0 & 0 & 0 \\ \frac{\partial N_i}{\partial y} & \frac{\partial N_i}{\partial x} & 0 & 0 & 0 \\ 0 & 0 & 0 & \frac{\partial N_i}{\partial x} & 0 \\ 0 & 0 & 0 & 0 & \frac{\partial N_i}{\partial y} \\ 0 & 0 & 0 & \frac{\partial N_i}{\partial y} & \frac{\partial N_i}{\partial x} \\ 0 & 0 & \frac{\partial N_i}{\partial x} & N_i & 0 \\ 0 & 0 & \frac{\partial N_i}{\partial y} & 0 & N_i \end{bmatrix} \tag{3.35}$$

Equation 3.30 is divided into a finite number of element domains, A_e, within the total domain A in such a way, that

$$\int_{t1}^{t2} \sum_{e=1}^{N_e} \int_{A_e} \left[\{\delta\overline{u}^e\}^T \left[\overline{M}\right] \left\{\ddot{\overline{u}}^e\right\} + \{\delta\overline{\epsilon}^e\}^T \left[\overline{D}\right] \{\overline{\epsilon}^e\}\right] dAdt \tag{3.36}$$

where N_e is the number of elements in the mesh

Substituting Equations 3.32 and 3.33 into the above equation, we get

$$\int_{t1}^{t2} \left[\sum_{e=1}^{N_e} \left(\{\delta a^e\}^T [M^e] \{a^e\} + \{\delta a^e\}^T [K^e] \{a^e\} \right) \right] dt = 0 \tag{3.37}$$

where

$$[M^e] = \int_{A_e} [N^e]^T \left[\overline{M}\right] [N^e] \, dA$$

$$= \int_{-1}^{+1} \int_{-1}^{+1} [N^e]^T \left[\overline{M}\right] [N^e] \, det\,[J] \, d\xi d\eta \tag{3.38}$$

$$[K^e] = \int_{A_e} [B^e]^T \left[\overline{D}\right] [B^e] \, dA$$

$$= \int_{-1}^{+1} \int_{-1}^{+1} [B^e]^T \left[\overline{D}\right] [B^e] \, det\,[J] \, d\xi d\eta \tag{3.39}$$

where $det\,[J]$ is the determinant of the standard Jacobian matrix and (ψ, η) are natural co-ordinates of the master element.

Finally, the element stiffness and mass matrices are assembled to get the global stiffness matrix $[K]$ and mass matrix $[M]$ as given below:

$$[K] = \int_0^a \int_0^b [B]^T \left[\overline{D}\right] [B] \, dxdy \tag{3.40}$$

and

$$[M] = \int_0^a \int_0^b [N]^T \left[\overline{M}\right] [N] \, dxdy \tag{3.41}$$

Using Hamilton's principle, we get the governing equation for free vibration of the plate as

$$[K] \{a\} - [M] \{a\} = 0 \tag{3.42}$$

Assuming harmonic oscillation,

$$a = A \sin \omega t$$

Using the above equation, Equation 3.42 can be written as.

$$[K]\{a\} + \omega^2 [M]\{a\} = 0 \tag{3.43}$$

where $\{a\}$ is the nodal displacement vector.

With the above formulation, analysis was done in MSC PATRAN package for the present problem.

The plate was clamped at both the edges along length-wise direction. Clamping was done with the help of "C" clamps. Analysis was done to get the first three normal modes of the plate and shown in Table 3.1.

Fig.3.2 shows the discretisation of the plate with QUAD4 isoparametric elements. The number of elements are 160 and number of nodes are 189. Each node has five degrees of freedom.

Fig.3.3 to Fig.3.5 shows the first, second and third modes of the plate under free vibration. The number 123456 in all these figures at the corners indicates that the translations (T1, T2, T3) and rotations (R1, R2, R3) are constrained along width-wise edges.

Fig.3.3 shows the first mode shape along length-wise direction. The maximum deformation is at node 11 and the value is 4.79 mm.

Fig.3.4 shows the second mode shape along the y-direction. The maximum deformation is at node 11 and the value is 7.79 mm.

Fig.3.5 shows the third mode shape along the x-direction. The maximum deformation is at node 7 and the value is 4.73 mm.

Table 3.1: REAL EIGEN VALUES OF THE PLATE

MODE NO.	EIGEN VALUE	RADIANS	CYCLES	GENERALIZED MASS	GENERALIZED STIFFNESS
1	1.092627E+06	1.045288E+03	1.663627E+02	1.000000E+00	1.092627E+06
2	3.809490E+06	1.951791E+03	3.106372E+02	1.000000E+00	3.809490E+06
3	8.404785E+06	2.899101E+03	4.614062E+02	1.000000E+00	8.404785E+06

Figure 3.2: MESHING OF PLATE

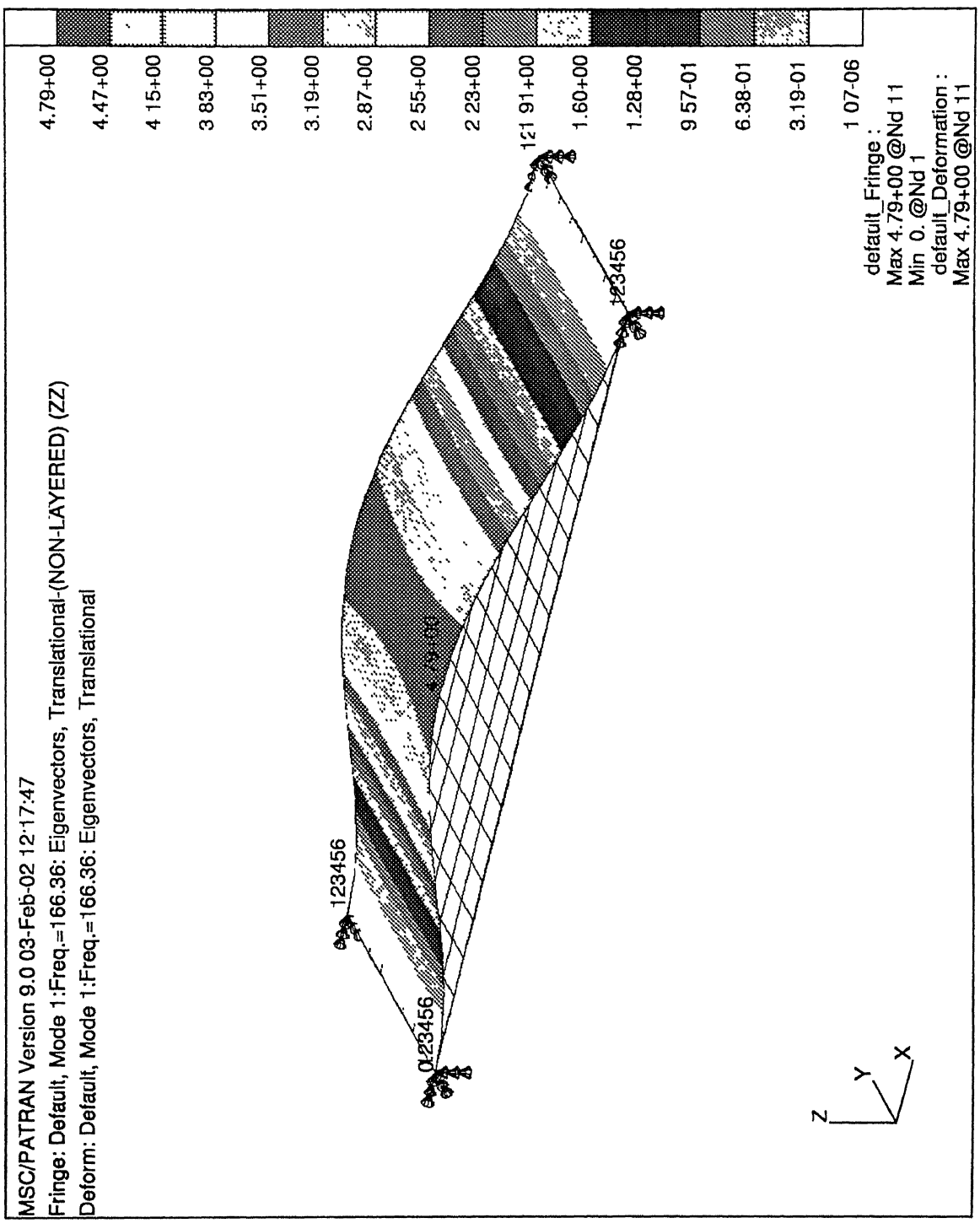

Figure 3.3: FIRST MODE OF PLATE

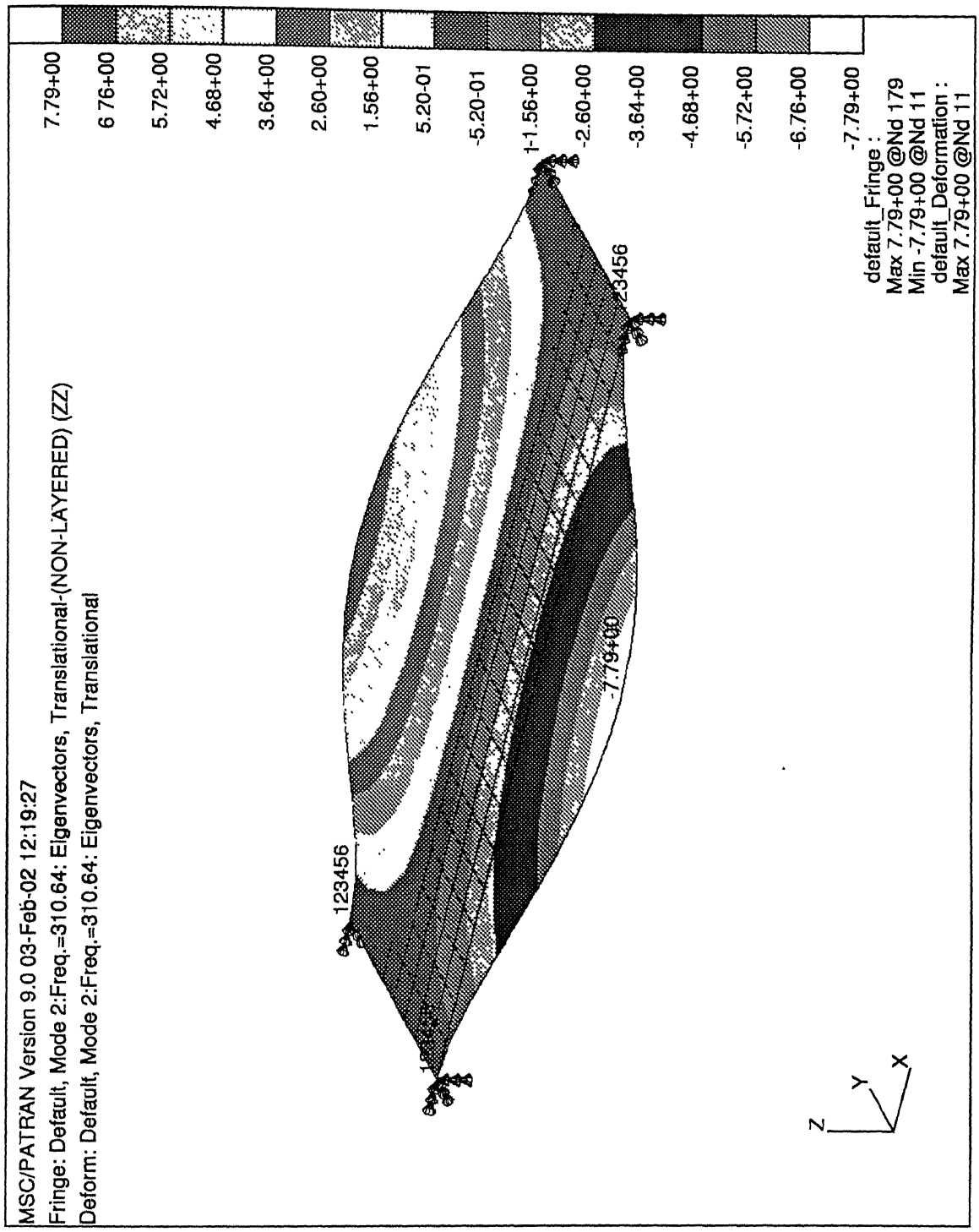

Figure 3.4: SECOND MODE OF PLATE

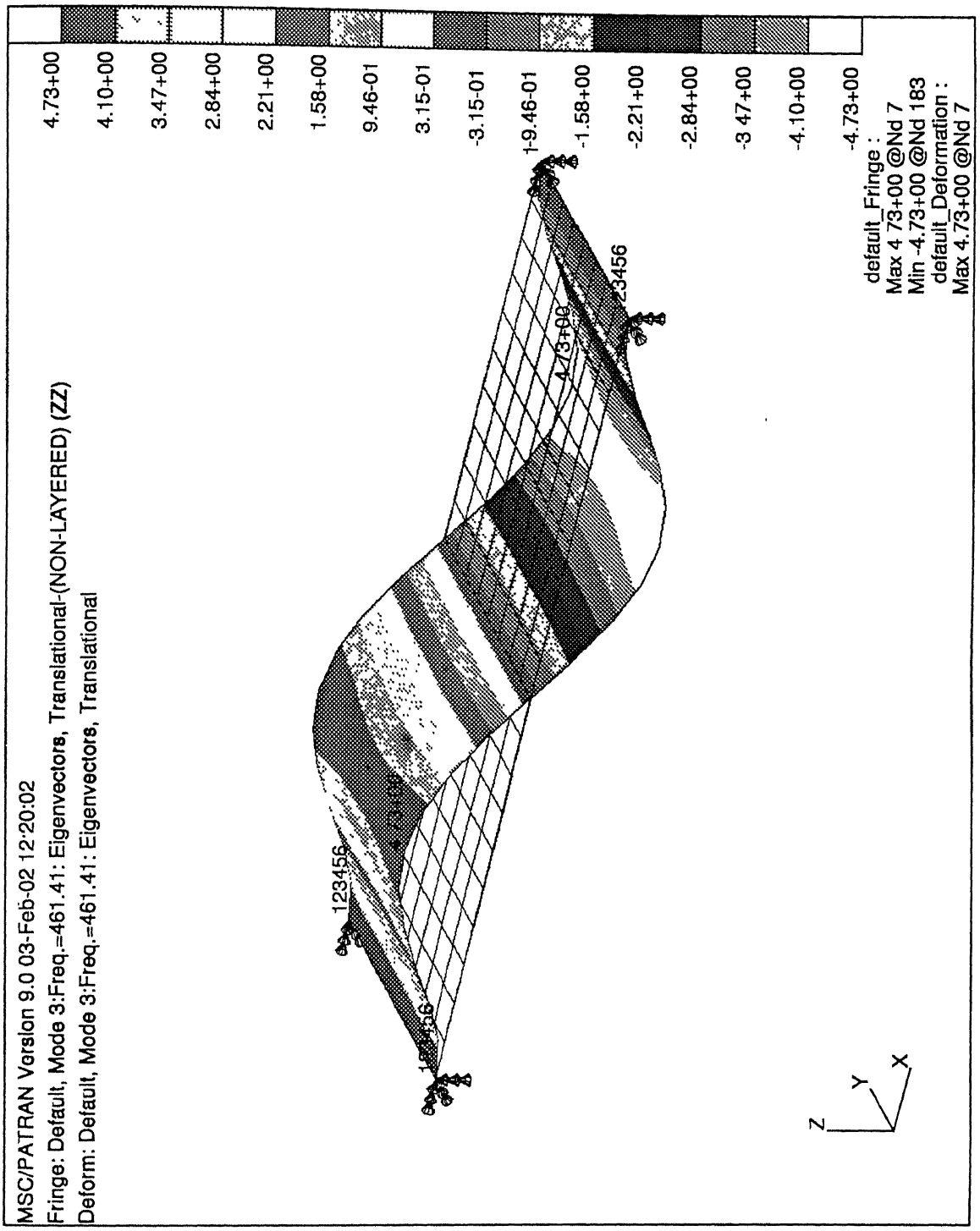

Figure 3.5: THIRD MODE OF PLATE

Chapter 4

FORMULATION OF BEAM VIBRATION RESPONSE

The objective of this analysis is to predict the displacement and acceleration response of the composite beam embedded with piezoelectric actuator. A cantilever beam shown in fig.4.1 was considered for this analysis. Crawley and Javier de Luis [7] presented one dimensional analysis for a cantilever beam embedded with piezoelectric actuators of size equal to beam width by considering the strain compatibility in the longitudinal direction. The present analysis extends this analysis by enforcing the strain compatibility in all directions and also considers finite size of the actuators.

Certain assumptions which were made for the theoretical formulation are:-

1. It was assumed that the actuators were perfectly bonded to the surrounding substructure and the strains in the actuators are compatible with the surrounding structure.

2. A linearly varying strain was assumed across the thickness of beam and actuator.

3. The strains developed in the crystals are within the elastic element.

Two actuators are placed at equal distances from neutral axis of the beam and the direction of the applied electric field along the thickness direction.

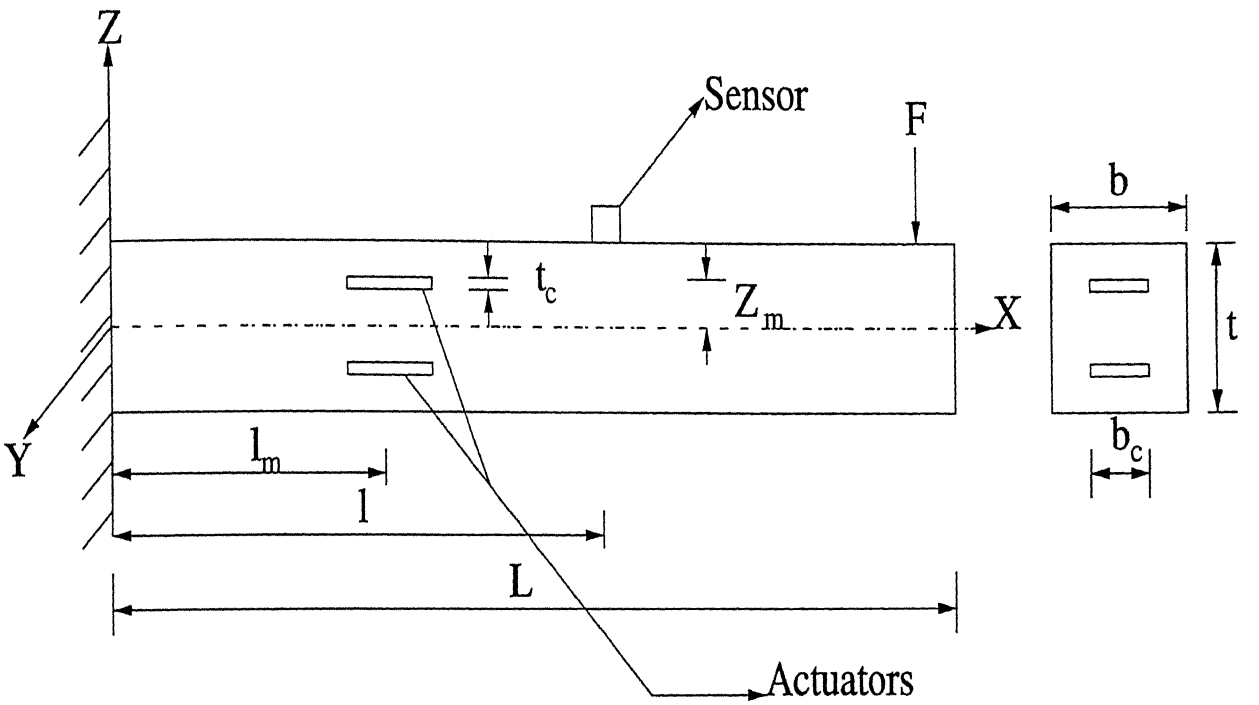

where

L = length of beam

l = location of sensor

l_m = location of actuators

b = width of beam

t = thickness of beam

b_c = width of crystal

t_c = thickness of crystal

Z_m = distance of mid-plane of the crystal from neutral axis of the beam

F = Applied force

Figure 4.1: CANTILEVER BEAM USED FOR DYNAMIC TEST

The beam was assumed to be a linear elastic structure so that the externally applied forces could be related to the acceleration, velocity or displacement vectors by means of linear influence coefficients. Any continuous structure is a system with infinite degrees of freedom, but to avoid the complicacies in mathematical modelling, it can be considered as a system with N degrees of freedom.

The lateral deflection $v(x,t)$ of any N degrees of freedom system can be approximated by the relation

$$v(x,t) = q_1(t)\varphi_1(x) + q_2(t)\varphi_2(x) + \ldots\ldots\ldots\ldots + q_N(t)\varphi_N(x) \tag{4.1}$$

where q_i $(i = 1, 2, \ldots\ldots, N)$ are generalised co-ordinates and φ_i $(i = 1.2, \ldots\ldots, N)$ are assumed dimensionless shape functions which satisfy the prescribed geometric boundary conditions. For the cantilever beam, the geometric boundary conditions are

$$v(x,t) = \frac{dv}{dx} = 0 \tag{4.2}$$

at the built-in end.

For the cantilever beam, φ_i is assumed to equal to $1 - \cos((2i-1)\frac{\pi x}{2L})$. Lagrange's equations of motion are

$$\frac{\partial}{\partial t}\left(\frac{\partial T}{\partial \dot{q}_i}\right) - \frac{\partial T}{\partial q_i} + \frac{\partial V}{\partial q_i} = Q_i \tag{4.3}$$

where T =Total kinetic energy

V = Total potential energy

$Q_i (i = 1, 2, \ldots., N)$ = generalised forcing functions

$q_i = q_1, q_2, \ldots\ldots, q_N$ are generalised coordinates respectively.

Thus

$$v(x,t) = \sum q_i\varphi_i = \sum q_i\left(1 - \cos((2i-1)\frac{\pi x}{2L})\right) \tag{4.4}$$

The total kinetic energy of the beam will be sum of the kinetic energy of the beam and kinetic energy of the sensor or accelerometer located at a

distance l from the built-in end.

Kinetic energy of the beam

$$T_1 = \int_0^L \frac{1}{2} m \left(\frac{dv}{dt}\right)^2 dx \tag{4.5}$$

where m = mass per unit length of the beam. Kinetic energy of the sensor is

$$T_2 = \frac{1}{2} m_s \left(\frac{dv}{dt}\right)^2 dx \tag{4.6}$$

at $x = l$, where m_s is the mass of the sensor.

Total kinetic energy

$$T = T_1 + T_2 \tag{4.7}$$

Substituting Eq.4.4 into Eq.4.5 and Eq.4.6,

$$T_1 = \frac{1}{2} m \int_0^L \sum_{i=1}^{N} \sum_{j=1}^{N} q_i q_j \left(1 - \cos\left(\frac{2i-1}{2L}\right)\pi x\right)\left(1 - \cos\left(\frac{2j-1}{2L}\right)\pi x\right) dx \tag{4.8}$$

$$T_2 = \frac{1}{2} m_s \sum_{i=1}^{N} \sum_{j=1}^{N} q_i q_j \left(1 - \cos\left(\frac{2i-1}{2L}\right)\pi l\right)\left(1 - \cos\left(\frac{2j-1}{2L}\right)\pi l\right) \tag{4.9}$$

Evaluating the above terms, we get

$$T = \sum_{i=1}^{N} \sum_{j=1}^{N} q_i q_j [\frac{m}{2} \left\{ L + \frac{2L}{(2i-1)\pi}(-1)^i + \frac{2L}{(2j-1)\pi}(-1)^j + \delta_{ij}\frac{L}{2} \right\} +$$

$$\frac{m_s}{2} \left\{ \left(1 - \cos\left(\frac{2i-1}{2L}\right)\pi l\right)\left(1 - \cos\left(\frac{2j-1}{2L}\right)\pi l\right) \right\}] \tag{4.10}$$

The total potential energy V will be

$$V = \frac{1}{2} E_B I_B \int_0^L \left(\frac{d^2 v}{dx^2}\right)^2 dx$$

$$V = \frac{1}{2} E_B I_B \sum_{i=1}^{N} \sum_{j=1}^{N} q_i q_j (2i-1)^2 (2j-1)^2 \left(\frac{\pi}{2L}\right)^4 \int_0^L \cos\left(\frac{2i-1}{2L}\right)\pi x \cos\left(\frac{2j-1}{2L}\right)\pi x dx$$

$$V = \frac{E_B I_B \pi^4}{64 L^3} \sum_{i=1}^{N} q_i (2i-1)^4 \tag{4.11}$$

To employ the Lagrange's principle, we need to know the virtual work done by the externally applied force 'F' at the tip of the beam. This can be calculated as

$$\delta W = F\,(\delta\theta)_{x=L}$$

$$(\delta\theta)_{x=L} = \left(\frac{dv}{dx}\right)_{x=L} (dq)_{x=L}$$

$$= \sum_{i=1}^{N} dq_i \left(\frac{2i-1}{2L}\right)\pi \sin\left(\frac{2i-1}{2L}\right)\pi L$$

$$\delta W = \sum_{i=1}^{N} F \delta q_i \left(\frac{2i-1}{2L}\right)\pi \sin\left(\frac{2i-1}{2L}\right)\pi L \tag{4.12}$$

the above expression of δW can be written as

$$\delta W = \sum_{i=1}^{N} Q_i \delta q_i$$

where

$$Q_i = F \left(\frac{2i-1}{2L}\right)\pi \sin\left(\frac{2i-1}{2L}\right)\pi L \tag{4.13}$$

Applying the Lagrange's equation to obtain the equation's of motion

$$\frac{\partial}{\partial t}\left(\frac{\partial T}{\partial \dot{q}_i}\right) + \frac{\partial V}{\partial q_i} = Q_i$$

The term $\left(\frac{\partial T}{\partial q_i}\right)$ is deleted as there is no term in kinetic energy equation which is a function of q_i.

$$\left(\frac{\partial T}{\partial\, q_i}\right) = \sum_{i=1}^{N}\sum_{j=1}^{N} q_j \left[\frac{m}{2}\left\{L + \frac{2L}{(2i-1)\pi}(-1)^i + \frac{2L}{(2j-1)\pi}(-1)^j + \delta_{ij}\frac{L}{2}\right\} +\right.$$

$$\left.\frac{m_s}{2}\left\{\left(1-\cos\left(\frac{2i-1}{2L}\right)\pi l\right)\left(1-\cos\left(\frac{2j-1}{2L}\right)\pi l\right)\right\}\right] +$$

$$\sum_{i=1}^{N}\sum_{j=1}^{N} \delta_{ij}\, \dot{q}_j \left[\frac{m}{2}\left\{L + \frac{2L}{(2i-1)\pi}(-1)^i + \frac{2L}{(2j-1)\pi}(-1)^j + \delta_{ij}\frac{L}{2}\right\} +\right.$$

$$\left.\frac{m_s}{2}\left\{\left(1-\cos\left(\frac{2i-1}{2L}\right)\pi l\right)\left(1-\cos\left(\frac{2j-1}{2L}\right)\pi l\right)\right\}\right] \qquad (4.14)$$

$$\frac{\partial}{\partial t}\left(\frac{\partial T}{\partial\, \dot{q}_i}\right) = \sum_{i=1}^{N}\sum_{j=1}^{N} \dot{q}_j \left[\frac{m}{2}\left\{L + \frac{2L}{(2i-1)\pi}(-1)^i + \frac{2L}{(2j-1)\pi}(-1)^j + \delta_{ij}\frac{L}{2}\right\} +\right.$$

$$\left.\frac{m_s}{2}\left\{\left(1-\cos\left(\frac{2i-1}{2L}\right)\pi l\right)\left(1-\cos\left(\frac{2j-1}{2L}\right)\pi l\right)\right\}\right] +$$

$$\sum_{i=1}^{N}\sum_{j=1}^{N} \delta_{ij}\, q_j \left[\frac{m}{2}\left\{L + \frac{2L}{(2i-1)\pi}(-1)^i + \frac{2L}{(2j-1)\pi}(-1)^j + \delta_{ij}\frac{L}{2}\right\} +\right.$$

$$\left.\frac{m_s}{2}\left\{\left(1-\cos\left(\frac{2i-1}{2L}\right)\pi l\right)\left(1-\cos\left(\frac{2j-1}{2L}\right)\pi l\right)\right\}\right] \qquad (4.15)$$

The above term in the right hand side can be written as $M_{ij}q_i$ where M_{ij} are the elements of the mass matrix whose values are given by

$$M_{ij} = \left[m\left\{\frac{3}{2} - \frac{4}{(2i-1)\,\pi}(-1)^i\right\} + m_s\left\{1-\cos\left(\frac{2i-1}{2L}\right)\pi l\right\}^2\right] \quad if\ i = j \qquad (4.16)$$

$$M_{ij} = [\frac{m}{2}\left\{1 + \frac{2}{(2i-1)\pi}(-1)^i + \frac{2}{(2j-1)\pi}(-1)^j\right\} +$$

$$\frac{m_s}{2}\left\{1 - \cos\left(\frac{2i-1}{2L}\right)\pi l\right\}\left\{1 - \cos\left(\frac{2j-1}{2L}\right)\pi l\right\}] \quad if\, i \neq j \tag{4.17}$$

The mass matrix is a symmetric square matrix of the order $n \times n$ and the off-diagonal terms are non zero. q_i is a vector of $n \times 1$ order which can be written as

$$\{q_i\}^T = \{q_1, q_2, ..., q_n\} \tag{4.18}$$

and

$$[M] = \begin{bmatrix} M_{11} & & & & \\ M_{21} & M_{22} & & & \\ .... & .... & & & \\ .... & .... & & & \\ M_{n1} & .... & .. . & .... & M_{nn} \end{bmatrix} \tag{4.19}$$

Similarily, the potential energy term differentiated with respect to q in the Lagrange's equation will give rise the stiffness matrix in which elements are given by the term

$$K_{ij} = \frac{E_B I_B \pi^4}{32L^3}(2i-1)^4 \delta_{ij} \tag{4.20}$$

where δ_{ij} is the Kronecker delta function. Substitution in terms of matrix will give the equation as

$$[M]\left\{\dot{q}\right\} + [K]\{q\} = \{Q\} \tag{4.21}$$

Natural frequencies of the beam can be calculated from the above equation by equating the forcing function to zero. So, for evaluating the natural frequencies, the equation will be

$$[M]\{\ddot{q}\} + [K]\{q\} = \{0\} \tag{4.22}$$

Substituting

$$\{q\} = \{A\}\sin(\omega_o t + \phi) \tag{4.23}$$

in above equation, gives

$$\begin{bmatrix} M_{11} & & & & \\ M_{21} & M_{22} & & & \\ .... & .. & & & \\ .... & .... & .... & & \\ M_{n1} & .... & .... & .... & M_{nn} \end{bmatrix} \begin{Bmatrix} A_1 \\ A_2 \\ .... \\ .... \\ A_n \end{Bmatrix} + \begin{bmatrix} K_{11} & & & & \\ 0 & K_{22} & & & \\ .. & .... & & & \\ .... & .... & ... & & \\ 0 & 0 & .... & .... & K_{nn} \end{bmatrix} \begin{Bmatrix} A_1 \\ A_2 \\ .... \\ .... \\ A_n \end{Bmatrix} \left(\frac{-1}{\omega_o^2}\right) = \{0\}$$

where $\{0\}$ is a $n \times 1$ order zero vector.

After premultiplying the above equation by $[K]^{-1}$, it can be written as

$$[K]^{-1}[M] \begin{Bmatrix} A_1 \\ A_2 \\ .... \\ .... \\ A_n \end{Bmatrix} = \left(\frac{1}{\omega_o^2}\right) \begin{Bmatrix} A_1 \\ A_2 \\ .... \\ .... \\ A_n \end{Bmatrix}$$

We now define a column vector

$$\left(\frac{1}{\omega_o^2}\right) = \begin{Bmatrix} \frac{1}{\omega_{o1}^2} \\ \frac{1}{\omega_{o2}^2} \\ .... \\ \frac{1}{\omega_{on}^2} \end{Bmatrix}$$

which is the eigen values vector of the matrix $[K]^{-1}[M]$

Corresponding to each of the eigen values, there will be an eigen vector. In order to decouple the equations of motion, the eigen vectors must be normalized. The normalizing procedure, which has been used here involves adjusting each modal amplitude $Z_r^{(i)}$, which satisfies the condition

$$\{Z_r\}^T [K] \{Z_r\} = 1 \tag{4.24}$$

where $Z_r^i = \frac{1}{c_r^i} \{A_r^i\}$ and $\{A_r^i\}$ is the eigen vector corresponding to the eigen value $\frac{1}{\omega_o^2}$

Corresponding to each eigen value of the set $\lambda_i (i = 1, 2, 3, ..., n)$ there will be a normalized eigen vector $Z_r^i (i = 1, 2, 3, ..., n)$.

c_r^i can be calculated for each eigen vector by making the substitution $Z_r^i = \frac{1}{c_r^i} \{A_r^i\}$.

A consequence of this type of normalizing together with the modal orthogonality relationships relative to the stiffness matrix is

$$\Phi^T K \Phi = I \tag{4.25}$$

where Φ is the complete set of N normalized mode shape vectors and I is a $n \times n$ identity matrix. The mode shapes normalized in this way are said to be orthonormal relative to the stiffness matrix.

Using the normalized vector, the equation

$$[M] \{A\} = [K] \{A\} \left(\frac{1}{\omega_o^2} \right)$$

can be written as

$$[M] \left\{ Z_r^1 \right\} = [K] \left\{ \frac{Z_r}{\omega_{o1}^2} \right\}$$

similar equations hold good for $\omega_{o2}, \omega_{o3}, ..., \omega_{on}$ with corresponding eigen vectors $\{A_i^2\}, \{A_i^3\}, ..., \{A_i^n\}$. In the matrix form, it can be written as

$$[M] \left[Z_r^1 \; Z_r^2 \qquad Z_r^n \right] = [K] \left[\frac{Z_r^1}{\omega_{o1}^2} \; \frac{Z_r^2}{\omega_{o2}^2} \qquad \frac{Z_r^n}{\omega_{on}^2} \right] \tag{4.26}$$

or

$$[M] [Z] = [K] [Z] [\Psi_o]$$

where

$$[\Psi_0] = \begin{bmatrix} \frac{1}{\omega_{o1}^2} & & & \\ & \frac{1}{\omega_{o2}^2} & & \\ & & & \\ & & & \frac{1}{\omega_{on}^2} \end{bmatrix}$$

Premultiplying Eq.4.26 by $[Z]^T$ gives

$$[Z]^T [M] [Z] = [Z]^T [K] [Z] [\Psi_o]$$

Substituting Eq.4.24 in above equation gives

$$[Z]^T [M] [Z] = [\Psi_o] \tag{4.27}$$

Introducing the transformation $\{q\} = [Z] \{p\}$ in the Eq.4.21 gives

$$[M] [Z] \left\{\ddot{q}\right\} + [K] [Z] \{p\} = \{Q\} \tag{4.28}$$

where $\{Q\} = \begin{Bmatrix} Q_1 \\ Q_2 \\ .... \\ Q_n \end{Bmatrix}$ is forcing function vector

we have $Q_i = F\left(\frac{2i-1}{2L}\right)\pi \sin\left(\frac{2i-1}{2L}\right)\pi l_m$ and forcing function $F = F_o \sin \omega t$
Premultiplying Eq.4.28 by $[Z]^T$

$$[Z]^T [M] [Z] \left\{q\right\} + [Z]^T [K] [Z] \{p\} = [Z]^T \{Q\}$$

Substituting Eq.4.24 and Eq.4.27 in the above equation, reduces to

$$[\Psi_o] \left\{\ddot{q}\right\} + \{p\} = [Z]^T \{Q\} \tag{4.29}$$

The equations are decoupled. the solution is

$$p_i = \left(\frac{1}{1 - \frac{\omega^2}{\omega_{oi}^2}} \right) \sum_{j=1}^{n} Z_{ji} \{Q\} \sin\omega t \tag{4.30}$$

Substituting back for $\{q\} = [Z]\{p\}$, we can calculate the displacement and acceleration in terms of generalised coordinate.

Experimental Procedure For Dynamic Test

Manufacture of glass/epoxy specimen

The smart glass/epoxy test specimen was prepared using plain woven glass fabric material. The dimensions of the test specimen, actuators and sensors are shown in Fig.4.1 and Table 4.1.

Embedding of PZT crystals

Leads of diameter 0.2 mm were flattened and attached to crystals on both faces by soldering. The overall thickness of the crystal along with leads is about 0.40 mm. So, to accommodate these crystals in the laminate, fibers from three lamina's were removed using a blade. Holes were 1 mm larger than the dimension of the PZT crystals and the crystals were inserted without causing any change in the nominal thickness of the laminate. Finally, the laminate was first cured at room temperature for 12 - 18 hours and then hot curing was followed. Aluminium end tabs were fixed to the beam at the clamping end on top and bottom to avoid delamination due to clamping.

Experimental Procedure for Dynamic Test

The specimen was clamped horizontally between steel plates. The base plate was welded to the fixed structure, specimen was placed on it and the top plate was tightened over the beam by bolts, which was effective in providing a cantilever boundary conditions. The natural frequency of the laminate was measured with the help of FFT Analyser for the first three modes and

Table 4.1: DYNAMIC TEST SPECIMEN DETAILS

	Material	Dimensions (mm)
Laminate	glass/epoxy	260 x 80 x 1.61
Crystal	PZT	10 x 10 x 0.25
Sensor	Endevco 2242C Accelerometer	Sensitivity 2.22 pc/g

were compared with the analytically predicted value. Analytically predicted values are shown in Table 4.2.

The beam is connected to a magnetic shaker through a connecting rod at the tip of the beam. The beam is subjected to concentrated time varying load. The forcing frequency was 65 Hz. The excitations of the beam were sensed by the embedded crystals. The output of the crystals was amplified by using a charge amplifier and measured with the help of FFT Analyser. The experimental set up is shown in Fig.4.2. The response of the PZT crystal and sensor is shown in Figs.4.3 & 4.4.

Table 4.2: REAL EIGEN VALUES OF THE CANTILEVER BEAM

MODE NO.	EIGEN VALUE	RADIANS	CYCLES	GENERALIZED MASS	GENERALIZED STIFFNESS
1	5.875284E+03	7.665040E+01	1.219929E+01	1.000000E+00	5.875284E+03
2	2.306334E+05	4.802430E+02	7.643305E+01	1.000000E+00	2.306334E+05
3	1.806803E+06	1.344174E+03	2.139319E+02	1.000000E+00	1.806803E+06

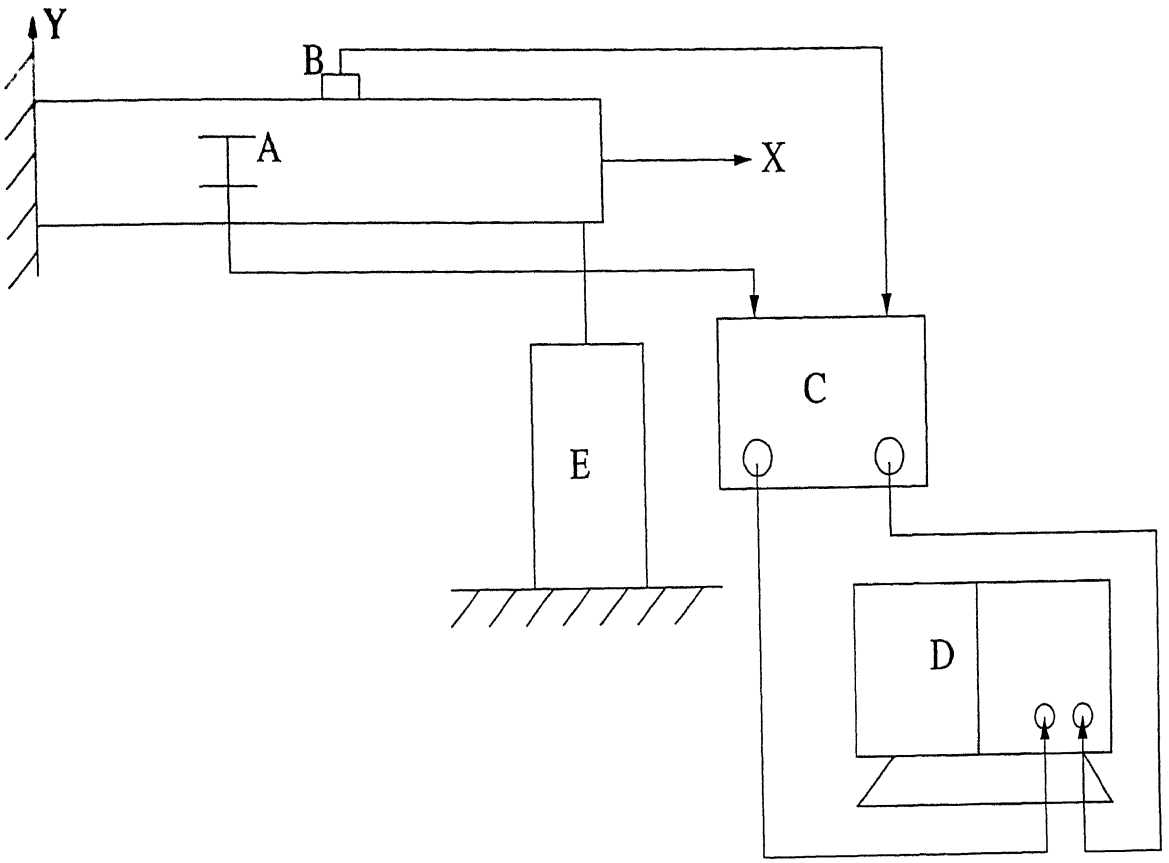

Where

A : PZT Crystals

B : Accelerometer

C : Charge Amplifier

D : FFT Analyser

E : Magnetic Shaker

Figure 4.2: SCHEMATIC DIAGRAM OF EXPERIMENTAL SET UP

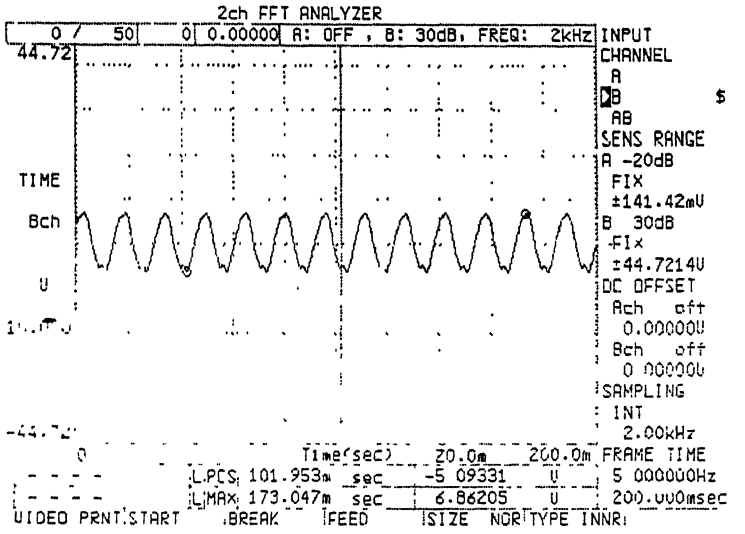

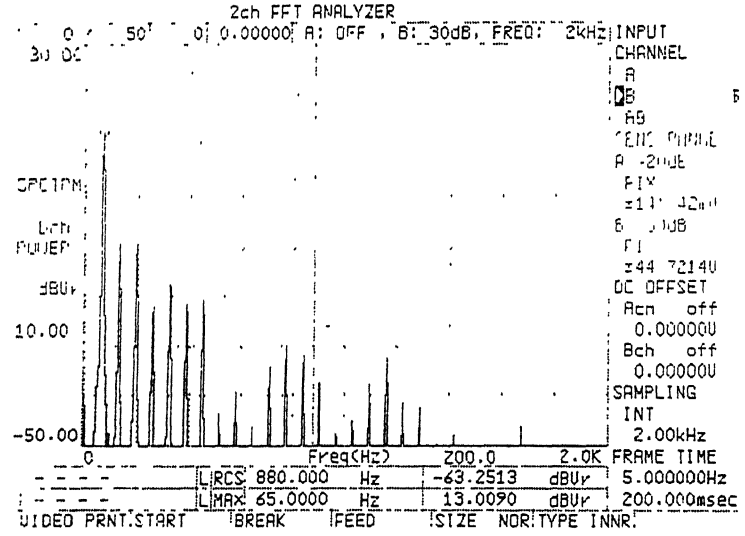

Figure 4.3: FORCED VIBRATION RESPONSE OF BEAM BY ACTUATOR

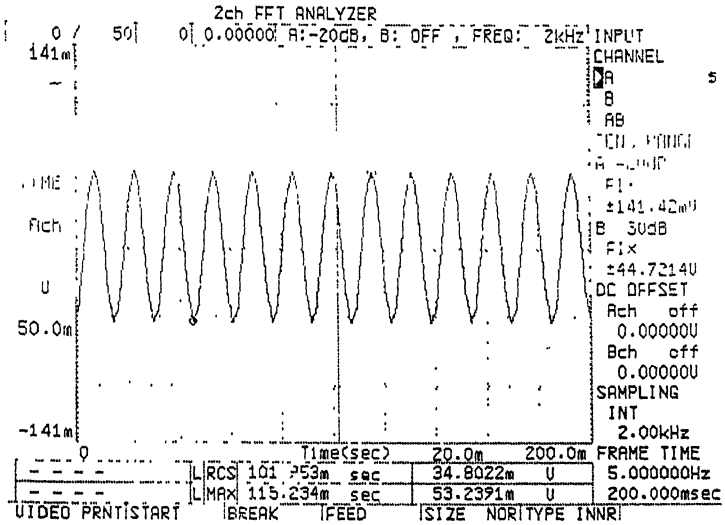

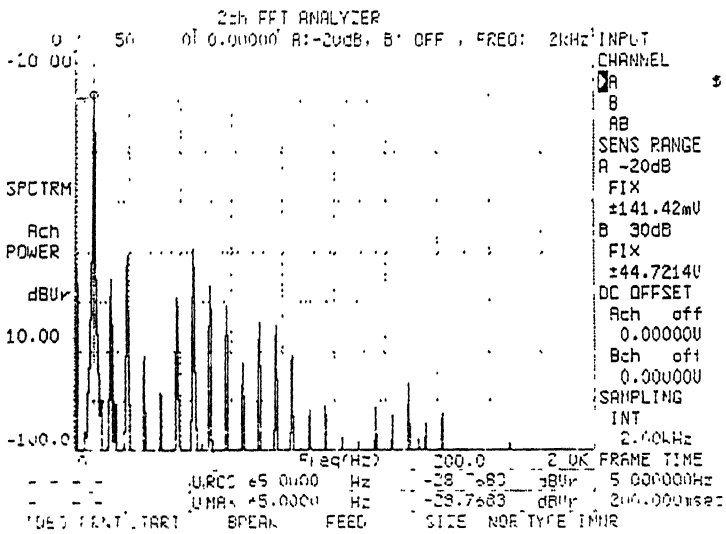

Figure 4 4: FORCED VIBRATION RESPONSE OF BEAM BY SENSOR

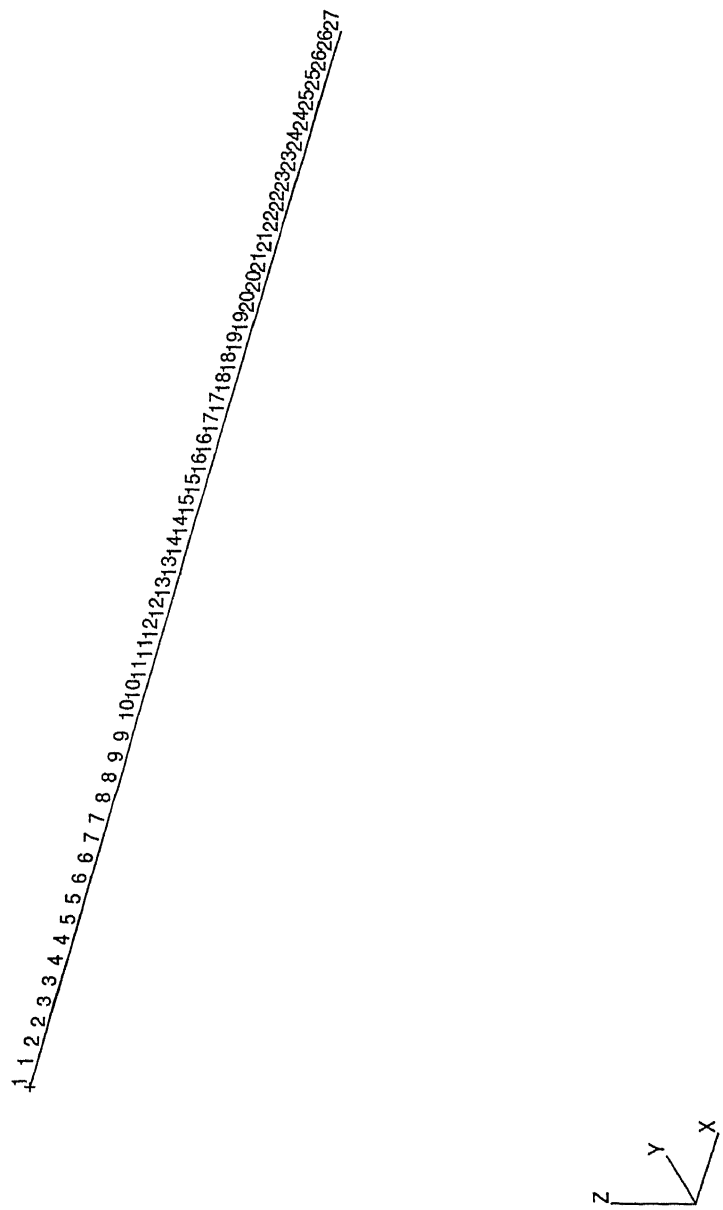

Figure 4.5: DISCRETISATION OF BEAM

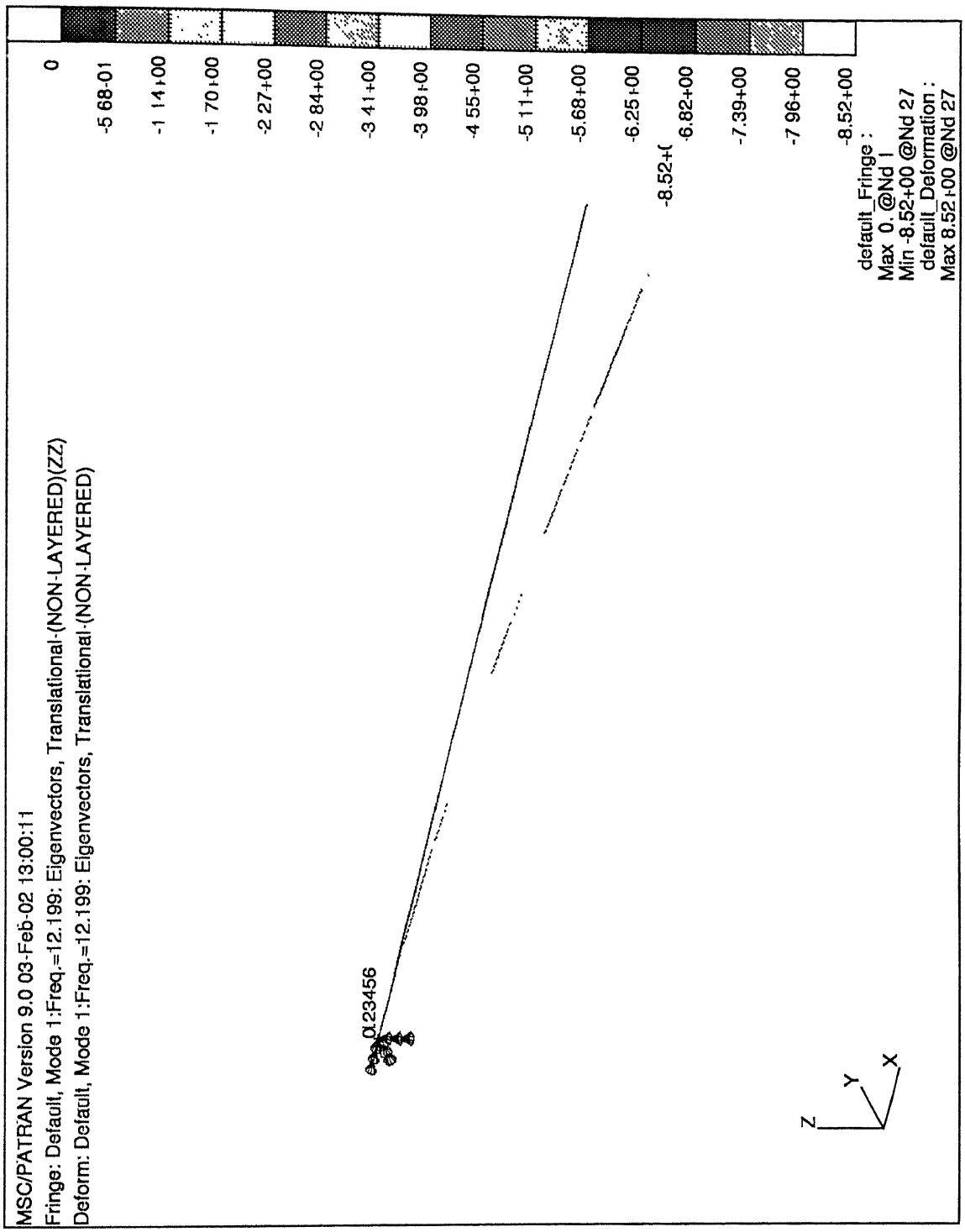

Figure 4.6: FIRST MODE OF BEAM

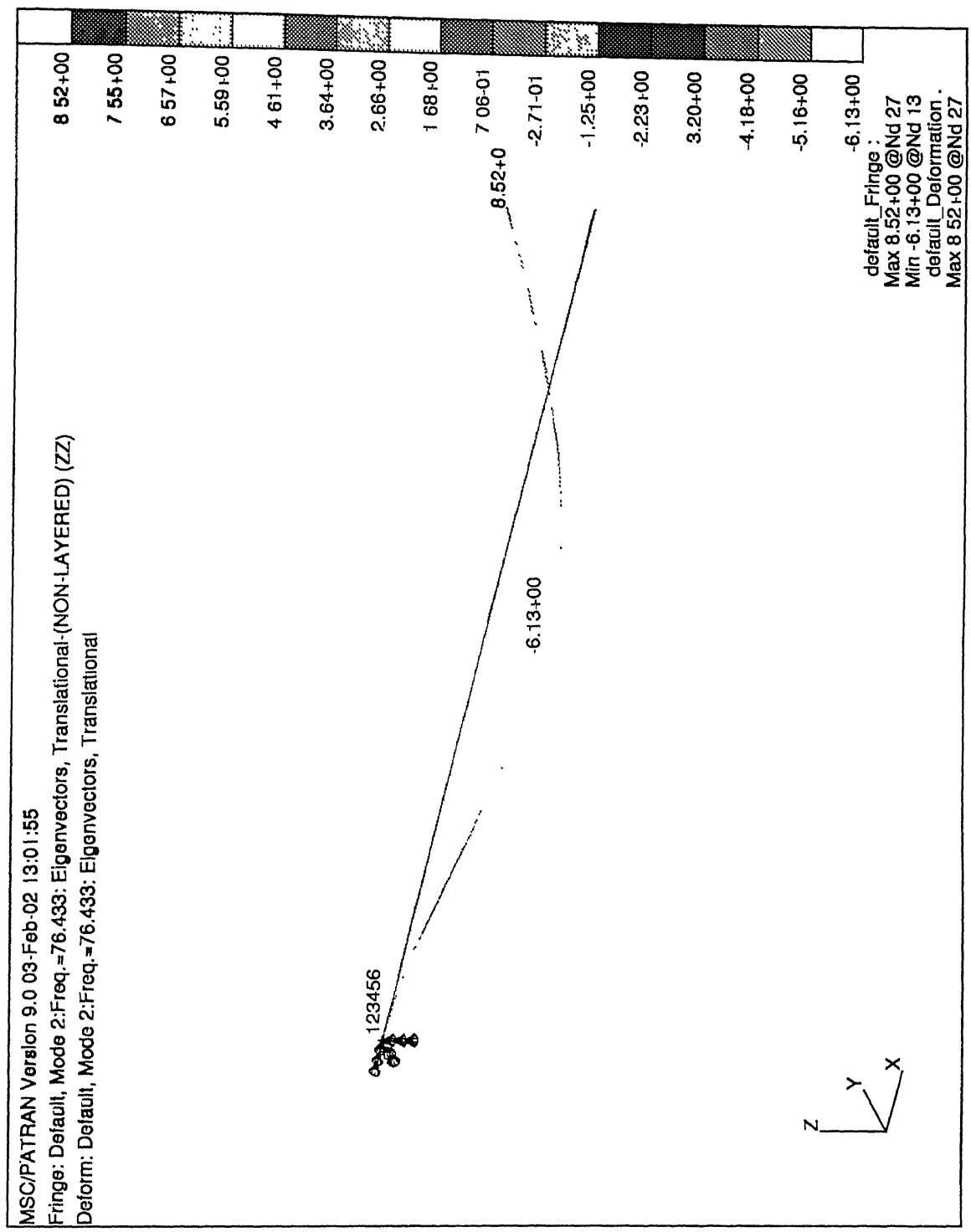

Figure 4.7: SECOND MODE OF BEAM

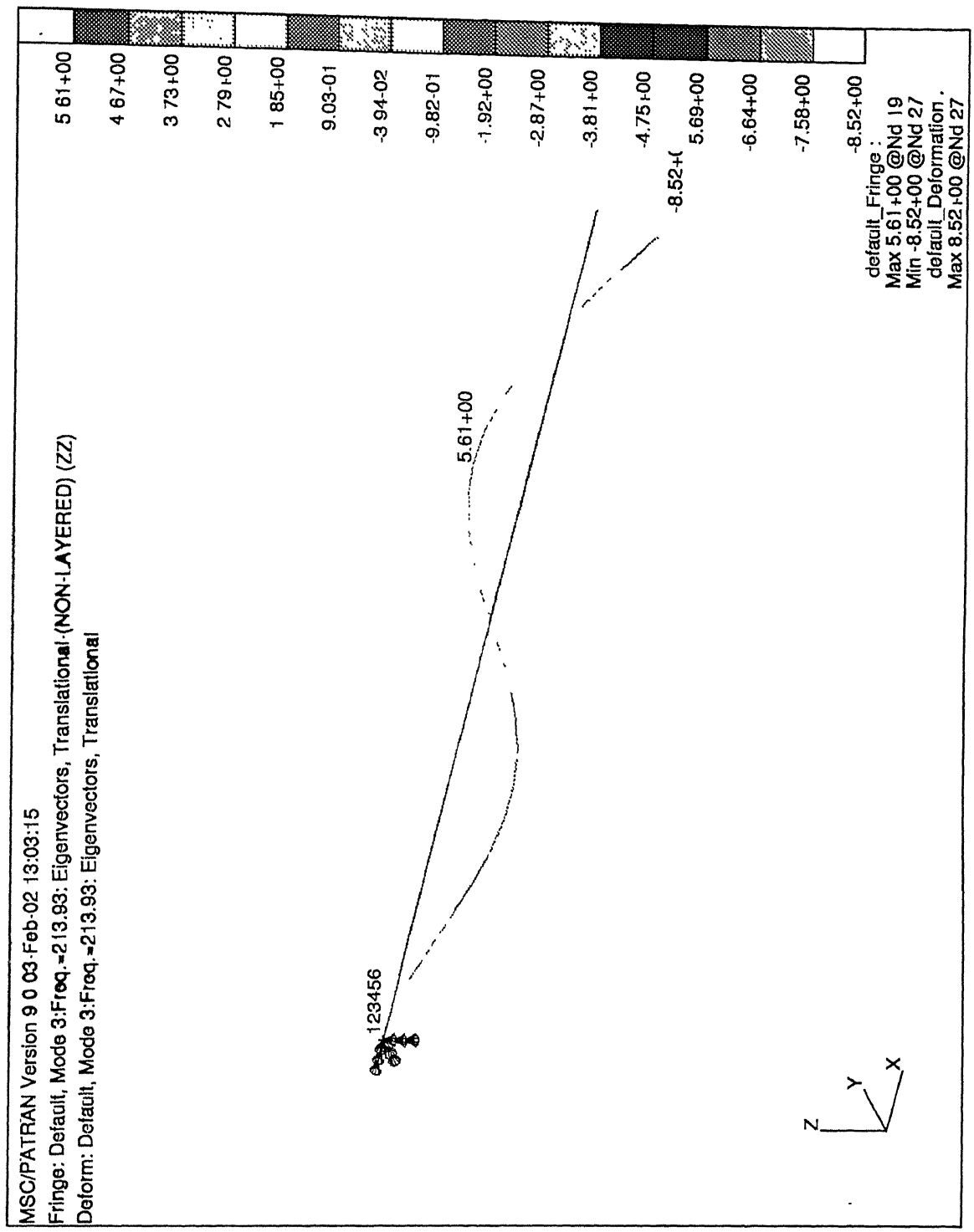

Figure 4.8: THIRD MODE OF BEAM

Chapter 5

RESULTS AND CONCLUSIONS

5.1 Composite Laminate

The composite laminates were prepared as described earlier. They were characterized for mechanical properties. The tensile test was carried out on a 10 ton MTS servo hydraulic machine. The Elastic modulus was found to be 5.776 GPa experimentally.The Burn out test was carried out to calculate the exact fiber volume fraction. The fiber volume fraction was found to be 0.46 and the rule of mixture was applied to calculate the Elastic modulus of the laminate. The value obtained by this method was 35.01 GPa. The poisson's ratio was found to be 0.22. Tensile tests were performed for two specimens on a table top tensile testing machine. The modulus was found to be 5.50 GPa.

The procedure suggested by Naik[22] was adopted to determine the moduli. The lamina was observed through a optical microscope to get the yarn width and gap width. Based on this information, the fiber volume fraction and poisson's ratio, the Elastic modulus and Shear modulus was found to be 16.50 GPa and 3.60 GPa respectively.

5.2 Dynamic Response

Natural frequency of the clamped - clamped plate and cantilever beam was measured theoretically and experimentally. Both the values for first three modes of the plate and beam are given in Tables 5.1 and 5.2 respectively. The experimental and theoretical acceleration of the sensor is shown in Table 5.3. The theoretical frequency modes of the plate and beam are shown in Figs.3.3 to 4.8.

5.3 Conclusions

MSC Patran was used for the analysis of both the plate and beam problem. The plate was meshed using Quad4 elements as shown in Fig.3.2. The analysis was carried for normal modes of the plate. The beam was discretised using Bar2 elements as shown in Fig.4.5. Sinusoidal loading ($F_o \sin \omega t$) was applied at the tip of the beam. The forcing frequency was 65 Hz. Analysis was done and the theoretical acceleration was found.

5.4 Future Work

With the experience gained in this work, one can address more complex structures such as plates and shells and can optimize for placements of actuators and sensors. The studies can be extended to close loop behaviour, where the response of the structure can be controlled through the complete cycle of sensing, processing of information and actuation.

Table 5.1: COMPARISON OF FIXED-FIXED PLATE NATURAL FREQUENCIES

Mode	Experimentally Predicted Frequency (Hz)	Theoretically Predicted Frequency (Hz)
First	165.00	166.36
Second	325.00	310.64
Third	475 00	461.41

Table 5.2: COMPARISON OF CANTILEVER BEAM NATURAL FREQUENCIES

Mode	Experimentally Predicted Frequency (Hz)	Theoretically Predicted Frequency (Hz)
First	22.50	12.20
Second	135.00	76.43
Third	275.00	213.93

Table 5.3: COMPARISON OF SENSOR ACCELERATION IN THE BEAM

Applied Force (N)	Experimentally Predicted	Theoretically Predicted
	Acceleration (m/sec^2)	Acceleration (m/sec^2)
50	52.024	65.250

Bibliography

[1] Gandhi,M.V. and Thompson,B.S. : Smart materials and structures, Chapman and Hall Publication, 1992.

[2] Rogers,A. Craig : Smart materials, structures, and mathematical issues, Technomic Publishing Company, inc., 620, 1991.

[3] Frank,M. and Janocha,H. : Smart materials - The IQ of materials in systems, Z.Metallkd., 87, 1996.

[4] Proceedings of international conference on smart materials, structures and systems, July 7-10,(1999), Bangalore, India, Allied Publishers Ltd , New Delhi.

[5] Crawley,E.F. Intelligent structures for Aerospace: A technology overview and assessment. AIAA Journal, 32(8):1689-1699, 1994.

[6] Hagood,N.W., Crawley,E.F , J.de Luis and Anderson,E.H. : Development of integrated components for control of intelligent structures, department of Aeronautics and Astronautics Building, MIT Cambridge MA 02139.

[7] Crawley F.Edward and Javier de Luis, "Use of piezoelectric actuators as elements of intelligent structures", AIAA Journal, vol.25 No.10, (1987),1373-1385

[8] Shen,Y.P., Wang,X.M. and Yin,L :Damage-monitoring in composite laminates by piezoelectric films, Computers and Structures, vol.59.

[9] Zhou,S., Liang,C. and Rogers,C.A. :Integration and design of piezoelectric element in intelligent structures, Journal of Intelligent Material Systems and Structures, vol.6, (1995), pp.733-743.

[10] Batra,R.C.,Liang,X.Q. and Yang,J.S. :Shape control of vibrating simply supported rectangular plates, AIAA Journal,vol.34,(1996),116-122.

[11] Lee,C.K., Journal of Acoustic Society of America,vol.87,No.3,March 1990, pp 1144-1158.

[12] Padma Akella, Xin Chen, Weiying Cheny, Declan Hughes and John T wen, "Modeling and Control of smart structures with bonded piezoelectric sensors and actuators", Smart Materials and Structures, 3(1994), pp 344-353.

[13] Hermen Shen,M.H., "Analysis of beams containing piezoelectric sensors and actuators", Smart Materials and Structures, 3(1994), pp 439-447.

[14] Chandrashekhara,K. and Agarwal,A.N., "Active vibration control of laminated composite plates using piezoelectric devices: A Finite Element Approach", Journal of Intelligent Material Systems and Structures, vol.4, Oct. 1993, pp 496-508.

[15] Liu,G.R.,Peng,X.Q.,Lam,K.Y., "Vibration control simulation of laminated comosite plates with integrated piezoelectrics", Journal of Sound and Vibration, (1999), 220(5), pp 827-846.

[16] ASTM Standards : Plastics Test Method - D 3039 - 76

[17] ASTM Standards : Standard Method of Test for Ignition Loss of Reinforced Resins - D 2584 - 68

[18] Yang,P.C., C.H.Norris and Y.Stavsky. 1966. "Elastic Wave Propagation in Heterogeneous Plates", International Journal of Solids and Structures, 2:665-684.

[19] Agarwal,B.D. and Broutman,J.L. Analysis and performance of fiber Composite Materials. John Wiley & Sons, Inc., New York, (1990).

[20] Jones,R.M. Mechanics of Composite Materials. McGraw-Hill, New York, (1975)

[21] Krishan K.Chawla : Composite Materials - Science and Engineering. Springer-Verlag Publications, (1987).

[22] Naik,N.K.,"Elastic behaviour of woven fabric composites: I - Lamina Analysis",Journal of Composite Materials,26(15),pp 2196-2225 (1992).

[23] Niranjan K.Naik : Woven Fabric Composites. Technomic Publishing Co.,Inc. Chapter 2.